

Energy-efficient flocking in multi-agent systems

Oleksandr Dykhovychnyi^{*†} Alexander Panchenko^{*‡}

Abstract

Modeling collective motion in multi-agent systems has gained much attention in recent years. In particular, of interest are the conditions under which flocking dynamics emerges. We present a generalization of the multi-agent model of Olfati-Saber [31] with non-linear navigational feedback forces. As opposed to the original model, our model is, in general, not dissipative. This makes obtaining sufficient conditions for flocking challenging due to the absence of an obvious choice of a Lyapunov function. By means of an alternative argument, we show that our model possesses a global attractor when the navigational feedback forces are bounded perturbations of the linear ones. We further demonstrate that, under mild conditions, the dynamics of the group converges to a complete velocity agreement at an exponential rate. We show that the attractor of a dissipative system can contain non-equilibrium solutions. We construct explicit examples of such solutions and obtain conditions under which they cannot exist. In addition, we present a case study of the energy efficiency of our model. We show how non-linear navigational feedback forces, which possess flexibility that linear forces lack, can be used to reduce on-board energy consumption.

1 Introduction

Swarming behavior is an essential characteristic of various biological systems, such as flocks of birds [23],[21], schools of fish [34],[22],[28], insect and bacteria colonies [7],[15],[42]. It often enables these groups of organisms to accomplish tasks that would be impossible for an individual organism to achieve on its own. For instance, a group of schooling fish can confuse a predator by making itself appear as a single organism [28], decreasing the likelihood of the group members being preyed upon. Such natural phenomena have inspired extensive research in the development of artificial multi-agent systems that possess swarm intelligence [17],[35]. One of the important examples of such systems is robotic swarms, which have recently received significant attention [2],[5],[46],[12],[56]. Robotic swarms, typically consisting of

^{*}Department of Mathematics and Statistics, Washington State University, Pullman, WA 99164, USA.

[†]o.dykhovychnyi@wsu.edu.

[‡]panchenko@wsu.edu.

relatively inexpensive and simple agents, offer high fault tolerance, cost-effectiveness, and scalability, which make them a promising tool for a broad range of tasks [40].

The applications of swimming robotic swarms range from injecting nano-scale robots into a human body for delivering drugs [11],[9] to using swarms of meter-scale autonomous underwater vehicles (AUV) to perform environment monitoring tasks in open water [39],[12]. For modeling this kind of system, it is crucial to take into account hydrodynamic effects of the medium a group operates in to accurately represent its true dynamics. The Dissipative Particle Dynamics (DPD) model, initially introduced in [24] as a coarse-grained particle-based simulation technique for fluids, has been successfully applied to modeling collective motion in systems like nanoswimmers [52],[55], active colloidal suspensions [33],[3], red blood cells [30],[18]. In the DPD model, the agents are represented as point masses that experience three types of short-range pairwise forces: *conservative* repulsive forces resulting from agent collisions, *dissipative* damping forces modeling viscous effects of the medium, and *random* forces representing stochastic effects. In active systems like [52],[55],[3],[3], the agents are also capable of producing a *self-propulsion* force. In the original DPD model [24], the dissipative force, dependent on the differences in agents' positions and velocities, is directed along the radial axis between two agents and only models the effect of extensional viscosity. Some later extensions of the model, such as [32], [27], also incorporate the effects of shear viscosity by introducing an analogous force in a transverse direction, providing a more realistic representation of the viscous effects of the surrounding medium.

Terrestrial and aerial robotic swarms find their application in agriculture [1], rescue operations [38],[20], reconnaissance for military operations [16], etc. In such systems, the effects of the medium are usually assumed to be negligible and the dynamics of an agent is determined solely by its control input. A common approach for mathematical modeling of such systems is based on the use of virtual forces [4]. In this approach, the control input of an agent is determined by solutions of the Newton's equations of motion, in which artificial forces, modeling agent interaction with the surrounding environment, involve measurements obtained from the agent's sensors rather than the true physical quantities. The popular model of Olfati-Saber (O-S) [31] is among the ones that are based on this approach. In this model, the velocity matching with the neighbors is achieved through the dissipative virtual force, and the spatial formation of the group is determined by the virtual conservative force derived from an attractive/repulsive potential. When the group is assigned a navigational objective to follow a given target trajectory (trajectory tracking problem), a virtual leading agent could be introduced in the model. By means of two additional *navigational feedback forces*, one of which is conservative and the other is dissipative, every agent in the group attempts to align its position and velocity with that of the virtual leader.

Since the motion of agents must be organized and coherent, an important feature of collective motion is *flocking*, a phenomenon when all members of the group move in the same direction with the same speed [51]. For some popular models of collective motion, the conditions under which flocking occurs are well-studied [50],[49],[31],[47],[14]. In particular, one of the characteristics that can lead to the emergence of flocking is *dissipativity*, a property of the system that its total mechanical energy is non-increasing in time [6]. This allows the

use of mechanical energy as a Lyapunov function to show the existence of a global attractor. In particular, the O-S model relies on this argument to demonstrate the presence of flocking. In the O-S model, the dynamics of the group is decoupled into the *translational dynamics* of the center of mass and the *structural dynamics* of the agents in a moving frame. With such a decomposition, the structural dynamics does not depend on the potentially arbitrary dynamics of the virtual leader and could be shown to be dissipative and converge to the set of equilibrium solutions having zero velocities relative to the center of mass, and hence representing flocking dynamics. However, the above decomposition relies on the fact that the navigational feedback forces are linear, which might not be flexible enough to implement an energy-efficient control. For instance, for small deviation from the target trajectory, it might be reasonable to relax (or entirely disable) control to save the on-board energy. In turn, large deviations from the target trajectory might be penalized more aggressively for the same purpose. The introduction of non-linear navigational feedback forces, however, makes the aforementioned decoupling problematic. Given that the coupled dynamics, in general, is not dissipative the conditions under which flocking can occur become unclear.

Although numerous developments of the O-S model have been proposed since its introduction, to the best of our knowledge, this issue has not been addressed yet. [44] considers the issue that, despite the guarantee that the agents in the O-S model will align their velocities with each other, it is unclear whether the common velocity would be the same as that of the virtual leader. By adding an additional virtual force that is equal to the virtual leader’s acceleration [44] make the complete dynamics dissipative, implying that the agents will asymptotically match their velocities with that of the virtual leader. However, the position- and the velocity-dependent terms in the navigational feedback forces remain linear. [36] extend the O-S model to the case of non-symmetric information exchange between agents and show that the presence of a spanning tree in the proximity graph of the group leads to flocking. [57] include a generic non-linear virtual force, describing intrinsic dynamics of an agent, that can potentially be coupled with both the virtual and the other followers in the group. However, the same term determines the dynamics of the virtual leader, so the model becomes similar to the one suggested in [41], and the Lyapunov-like argument could be applied. [43] study the case when only a fraction of agents have information about the virtual leader. The agents stay close to each other due to the infinite pairwise attractive potential, and only a single informed agent is enough to make the other agents follow the virtual leader through short-range dissipative interactions. [53] assumes that the agents have only intermittent measurements of the coordinates of the other agents, and [25] consider the case when the information between agents is exchanged with delays.

In this paper, we consider the problem of trajectory tracking for nanometer- to millimeter-scale swimming robots operating in water. We use the DPD model to simulate interactions of the agents mediated by the ambient environment. We assume that the agents are capable of self-propulsion, the direction and the magnitude of which are determined by means of non-linear virtual forces analogous to the navigational feedback forces in the O-S model. Treating the conservative and the dissipative forces in the DPD model as virtual, our model could be seen as a generalization of the O-S model with navigational feedback being non-

linear. Although the physical nature of the two models is different, the resulting dynamics of the agents is the same.

Our main contributions are as follows. First, for the target trajectories yielding dissipative dynamics, we show that the attractor determined by a Lyapunov function could contain non-equilibrium solutions. We provide explicit examples of such solutions and obtain broad sufficient conditions under which such solutions could not exit. Next, for a general case of non-dissipative dynamics with navigational feedback forces that are bounded perturbations of the linear ones, we obtain bounds on the agents' trajectories deviations from that of the virtual leader and show the existence of a global attractor. We further show that for some special configurations of the navigational feedback forces the agents' velocities asymptotically match at an exponential rate. Finally, by means of numerical simulations, we study how the non-linear navigational feedback forces might be configured to deliver energy-efficient dynamics.

The rest of the paper is organized as follows. In Section 6, we set up our model and describe the forces that determine the dynamics of the group. In Section 3, we obtain an attractor for the case when the dynamics becomes dissipative due to particular choices of the target trajectories. In Section 4, we study the existence of non-equilibrium solutions in such an attractor. In Section 5, we consider the general case of non-dissipative dynamics and obtain conditions under which the system exhibits asymptotic flocking. In Section 6, we present numerical simulations illustrating the flocking dynamics in our system under different regimes of motion. Finally, in Section 7, we numerically solve an optimal control problem to determine configurations of the navigational feedback forces that are energy-efficient.

2 Model of collective motion

Consider a group of N identical sphere-shaped agents submerged in water. The size of an agent is assumed to be in the range $10\mu\text{m}$ - 1mm . Each agent is equipped with a miniature propeller that allows it to steer itself in a desired direction. The direction and the magnitude of the propulsion are determined by means of an on-board processor based on the information about the agent's position and velocity as well as its navigational objective that are received from on-board sensors. The agents are also equipped with elastic bumpers preventing them from mechanical damage in case of collisions. For agents of the specified size range moving in water, the dynamics is characterized by a low Reynolds number (see, e.g., [41]), and therefore viscous forces created by the ambient environment must be taken into account.

Modeling agents as point masses, the dynamics of the group could be described by the following Newton's equations of motion:

$$\begin{aligned}\dot{\mathbf{q}}_i &= \mathbf{v}_i, \\ M\dot{\mathbf{v}}_i &= \sum_{j \neq i} \mathbf{f}_{ij}^C + \sum_{j \neq i} \mathbf{f}_{ij}^D + \mathbf{u}_i, \quad i = 1, \dots, N,\end{aligned}\tag{1}$$

where M is the mass of an agent, $\mathbf{q}_i(t), \mathbf{v}_i(t) \in \mathbb{R}^d, t \geq 0, d \in \{2, 3\}$, are the position and the velocity of the i -th agent, respectively, \mathbf{f}_{ij}^C and \mathbf{f}_{ij}^D are the conservative and the dissipative

ambient forces acting on the i -th agent due to its proximity to the j -th agent, and \mathbf{u}_i is the self-propulsion force generated by the i -th agent's propeller.

Remark 1. Aside from the conservative and the dissipative terms, the original DPD model [24] also includes terms representing stochastic effects in the agents' interactions. Here, we consider the scenarios with high Peclet number, that are characterized by the dominance of convective forces, so the stochastic effects might be neglected. However, some of the key results about the emergence of flocking dynamics presented in Section 5 will still hold in case a certain class of random forces is added to the model (see Remark 9).

Ambient forces. Both the conservative and the dissipative ambient forces are *pairwise short-range* forces meaning that they act on a given agent only if there is another agent located sufficiently close to it.

For two agents that are sufficiently close, either the resistance of the volume of water contained between the agents or the repulsion resulting from physical contact of their elastic bumpers induces the conservative *repulsive* force. The force is given by

$$\mathbf{f}_{ij}^C(\mathbf{q}_{ij}) = Aw_C(|\mathbf{q}_{ij}|)\mathbf{q}_{ij}, \quad i, j = 1, \dots, N, i \neq j,$$

where $A > 0$ is constant, $w_C : \mathbb{R}_{\geq 0} \rightarrow [0, 1]$ is a non-increasing C^1 weight function that vanishes on $[r_C, \infty)$, for some $r_C > 0$, and $\mathbf{q}_{ij} = \mathbf{q}_i - \mathbf{q}_j$. The value of r_C is assumed to be close to the diameter of an agent and is referred to as the *cut-off distance* of the conservative force. The sum of all conservative forces acting on the i -th agent is assumed to be the negative gradient of the collective repulsive potential $U(\mathbf{Q})$, where $\mathbf{Q} = (\mathbf{q}_1, \dots, \mathbf{q}_N)$, and we can write it as

$$\mathbf{f}_i^C = \sum_{j \neq i} \mathbf{f}_{ij}^C = -\nabla_{\mathbf{q}_i} U(\mathbf{q}).$$

Following [15],[37], we assume that the dissipative force, resulting from viscous interaction between nearby agents and the ambient environment, is given by

$$\mathbf{f}_{ij}^D(\mathbf{q}_{ij}, \mathbf{v}_{ij}) = -Bw_D(|\mathbf{q}_{ij}|)\mathbf{v}_{ij}, \quad i, j = 1, \dots, N, i \neq j,$$

where $B > 0$ is constant, $w_D : \mathbb{R}_{\geq 0} \rightarrow [0, 1]$ is a non-increasing C^1 function vanishing on $[r_V, \infty)$, for some cut-off distance $r_V > 0$, and $\mathbf{v}_{ij} = \mathbf{v}_i - \mathbf{v}_j$.

Note that both ambient forces are symmetric in the sense that $\mathbf{f}_{ji}^C = -\mathbf{f}_{ij}^C$ and $\mathbf{f}_{ji}^D = -\mathbf{f}_{ij}^D$, for all $i \neq j$.

Self-propulsion forces. The common navigational objective of the group is to move along a specified *target trajectory*, maintaining a *flock formation*. Here, we assume that the group is in a flock formation if all agents are moving with approximately the same velocity and the group is staying cohesive. The target trajectory is defined in the form of the *virtual leading agent* with coordinates $\mathbf{q}_l(t)$, $\mathbf{v}_l(t) \in \mathbb{R}^d$, $t \geq 0$, $l = N + 1$, that are updated according to

$$\dot{\mathbf{q}}_l = \mathbf{v}_l, \quad \dot{\mathbf{v}}_l = \mathbf{f}^L(t), \tag{2}$$

where $\mathbf{f}^L : [0, \infty) \rightarrow \mathbb{R}_{\geq 0}$ is C^1 . The non-linear self-propulsion force produced by an agent is the navigational feedback force, intended to align the agent's coordinates with the ones of the virtual leader, is given by

$$\mathbf{u}_i = \mathbf{u}^P(\mathbf{q}_{il}) + \mathbf{u}^V(\mathbf{v}_{il}), \quad i = 1, \dots, N. \quad (3)$$

In the above, the first term penalizes for an agent's position deviation from the position of the virtual leader and is defined by

$$\mathbf{u}^P(\mathbf{q}_{il}) = -h(|\mathbf{q}_{il}|) \mathbf{q}_{il}. \quad (4)$$

We would refer to (4) as the *position alignment self-propulsion force*. In turn, the second term in (3) penalizes for an agent's velocity deviation from that of the virtual leader, and is defined by

$$\mathbf{u}_i^V = \mathbf{u}^V(\mathbf{v}_{il}) = -g(|\mathbf{v}_{il}|) \mathbf{v}_{il}. \quad (5)$$

(5) would be referred to as the *velocity alignment self-propulsion force*. The functions h, g , referred to as *generating functions* of the corresponding forces, are given by

$$h(s) = \begin{cases} 0, & 0 \leq s \leq r_0, \\ \alpha \frac{k(s)}{s}, & s > r_0, \end{cases}, \quad g(s) = \begin{cases} 0, & 0 \leq s \leq v_0, \\ \beta \frac{p(s)}{s}, & s > v_0, \end{cases} \quad (6)$$

where $\alpha, r_0, \beta, v_0 \geq 0$ are tunable control parameters, and the functions $k : (r_0, \infty) \rightarrow \mathbb{R}_{>0}$ and $p : (v_0, \infty) \rightarrow \mathbb{R}_{>0}$ are increasing and such that h and g are C^1 .

Remark 2. Varying α and β in (6) allows to amplify the effects of the position alignment and the velocity alignment forces, respectively. Meanwhile, r_0 and v_0 make it possible to “relax” the control by turning the propulsion off when the deviation from the target trajectory is sufficiently small. In particular, when $r_0 > 0$, the agents are forced to stay within the ball of radius r_0 centered at $\mathbf{q}_l(t)$. In case the group is sufficiently large and r_0 is small enough so that the ambient dissipative force acts on the agents, its damping effect is leveraged to align agents' velocities. In this way, the agents' power consumption might be reduced. A detailed discussion of the effect of parameters r_0 and v_0 on the agents' dynamics is presented in Sections 6 and 7.

The position alignment force is conservative, so we can write it as

$$-h(|\mathbf{q}_{il}|) \mathbf{q}_{il} = -\nabla_{\mathbf{q}_i} \Phi(\mathbf{Q}, \mathbf{q}_l),$$

where Φ is a virtual attractive potential. In addition, it follows from the definition of $h(s)$ that Φ is at least C^1 and satisfy

$$\lim_{|\mathbf{q}_{il}| \rightarrow \infty} \Phi(\mathbf{Q}, \mathbf{q}_l) = \infty, \quad i = 1, \dots, N. \quad (7)$$

Remark 3. The model presented above is different from the O-S model in the following two aspects. First, our navigational feedback forces are, in general, non-linear, and the linear forces of the O-S model represent a partial case of ours with $k(s) = s$, $p(s) = s$, $r_0 = v_0 = 0$ set in (6). Second, whereas our conservative force is purely repulsive, the conservative force in the O-S model is repulsive only at small distances and becomes attractive at larger ones. Although this difference does not technically allow us to claim that our model is more general than the O-S model, this aspect of the conservative is not relevant for establishing the existence of flocking neither in [31] nor in our further discussion. Thus, the results presented in Sections 3, 3, 5 will apply to the O-S model without any additional modifications. The fact the short-range conservative force is both repulsive and attractive is used in [31] to ensure a certain spatial structure of the flock (α -lattice), however, its overall cohesion is rather guaranteed by the position-dependent navigational feedback force.

Proximity graph and vector form of the dynamics. Define the *proximity graph* [8] of the group as an undirected weighted graph $\mathcal{G}(\mathbf{Q}) = (\mathcal{A}, \mathcal{E}(\mathbf{Q}), \sigma)$, with $\mathcal{A} = \{1, \dots, N\}$, $\mathcal{E}(\mathbf{Q}) = \{(i, j) \in \mathcal{A} \times \mathcal{A} : |\mathbf{q}_{ij}| \leq r_D\}$, and $\sigma(i, j) = Bw_D(|\mathbf{q}_{ij}|)$. Then, the sum of all ambient dissipative forces acting on the i -th agent can be written as $\sum_{j \neq i} \mathbf{f}_{ij}^D = d_i \mathbf{v}_i - \sum_{j \neq i} a_{ij} \mathbf{v}_j$, where d_i is the degree of the i -th vertex of \mathcal{G} , and a_{ij} is the (i, j) -th element of its adjacency matrix. Letting $\mathcal{L}(\mathbf{Q})$ denote the Laplacian of $\mathcal{G}(\mathbf{Q})$ and $L(\mathbf{Q}) = \mathcal{L}(\mathbf{Q}) \otimes I_d$, where I_d is the $d \times d$ identity matrix, we can write the governing equations (1) in the following vector form

$$\begin{aligned} \dot{\mathbf{Q}} &= \mathbf{V}, \\ M\dot{\mathbf{V}} &= -\nabla_{\mathbf{Q}} U(\mathbf{Q}) - L(\mathbf{Q})\mathbf{V} - \nabla_{\mathbf{Q}} \Phi(\mathbf{Q}, \mathbf{q}_l) - G(\mathbf{V} - \mathbf{1}_N \otimes \mathbf{v}_l)(\mathbf{V} - \mathbf{1}_N \otimes \mathbf{v}_l), \end{aligned} \quad (8)$$

where $\mathbf{V} = (\mathbf{v}_1, \dots, \mathbf{v}_N)$, $G(\mathbf{V}) = \text{diag}(g(|\mathbf{v}_{1l}|), \dots, g(|\mathbf{v}_{Nl}|)) \otimes I_d$, and $\mathbf{1}_N$ is an N -dimensional vector of all ones. Note that the right-hand side of (8) depends on $\mathbf{q}_l(t)$, $\mathbf{v}_l(t)$, so, in general, the system (8) is non-autonomous.

3 Dissipative dynamics

In this section, our goal is to describe the asymptotic behavior of the system for the case when the navigational objective is to move with a constant velocity in a specified direction. This is one of the simplest possible target trajectories, yet it is typical for many scenarios. Furthermore, a wide range of more complex trajectories could be represented by a sequence of such simple trajectories. We are interested in determining whether the system exhibits flocking dynamics which we formally define as follows.

Definition 1. (a) The group of agents is said to exhibit (**approximate**) **flocking** if there exist $r, v > 0$ and $T \geq 0$, such that

$$|\mathbf{q}_i(t) - \mathbf{q}_j(t)| \leq r, \quad (9a)$$

$$|\mathbf{v}_i(t) - \mathbf{v}_j(t)| \leq v, \quad (9b)$$

for all $i, j = 1, \dots, N$ and all $t \geq T$. If, in addition,

$$|\mathbf{v}_v(t) - \mathbf{v}_j(t)| \rightarrow 0, \quad (10)$$

for all $i, j = 1, \dots, N$, we say that the group exhibits **exact flocking**.

(b) The group of agents is said to exhibit **(approximate) proper flocking** if there exist $R, V > 0$ and $T \geq 0$, such that

$$|\mathbf{q}_i(t) - \mathbf{q}_l(t)| \leq R, \quad (11a)$$

$$|\mathbf{v}_i(t) - \mathbf{v}_l(t)| \leq V, \quad (11b)$$

for all $i, j = 1, \dots, N$ and all $t \geq T$. If, in addition,

$$|\mathbf{v}_i(t) - \mathbf{v}_l(t)| \rightarrow 0, \quad (12)$$

for all $i = 1, \dots, N$, we say that the group exhibits **exact proper flocking**.

Note that while part (b) of the above definition requires the group to follow the virtual leader, part (a) allows the group to ignore the navigational objective.

If $\mathbf{f}^L(t) \equiv \mathbf{0}$, the navigational objective of the group becomes movement in the direction $\mathbf{v}_l(0)$ with a constant speed. In this case, the system becomes purely dissipative, and the standard Lyapunov-like argument can be applied to describe its asymptotic behavior [31].

For further development, it would be convenient to introduce a coordinate system centered at the coordinates of the virtual leader (moving frame coordinates). Let

$$\mathbf{x}_i = \mathbf{q}_i - \mathbf{q}_l, \quad \mathbf{w}_i = \mathbf{v}_i - \mathbf{v}_l, \quad i = 1, \dots, N,$$

and $\mathbf{X} = (\mathbf{x}_1, \dots, \mathbf{x}_N)$, $\mathbf{W} = (\mathbf{w}_1, \dots, \mathbf{w}_N)$. Since $\mathbf{x}_i - \mathbf{x}_j = \mathbf{q}_i - \mathbf{q}_j$ and $\mathbf{w}_i - \mathbf{w}_j = \mathbf{v}_i - \mathbf{v}_j$, for all $i, j = 1, \dots, N$, the governing equations could be written as

$$\begin{aligned} \dot{\mathbf{X}} &= \mathbf{W}, \\ M\dot{\mathbf{W}} &= -\nabla_{\mathbf{X}}U(\mathbf{X}) - L(\mathbf{X})\mathbf{W} - \nabla_{\mathbf{X}}\Phi(\mathbf{X}) - G(\mathbf{W})\mathbf{W} - M\mathbf{f}^L \otimes \mathbf{1}_N. \end{aligned} \quad (13)$$

In the above coordinate system, the group will exhibit exact proper flocking if $|\mathbf{W}(t)| \rightarrow \mathbf{0}$ as $t \rightarrow \infty$, and $|\mathbf{X}(t)| \leq R$, $t \geq T$, for some $R, T \geq 0$. If $|\mathbf{W}(t)|$ merely stays bounded for $t \geq T$, then the proper flocking would be approximate.

Let

$$E(\mathbf{X}, \mathbf{W}) = \frac{1}{2}M|\mathbf{W}|^2 + U(\mathbf{X}) + \Phi(\mathbf{X}) \quad (14)$$

be the total mechanical energy of (13). Then

$$\frac{d}{dt}E(\mathbf{X}(t), \mathbf{W}(t)) = -\mathbf{W}^T L(\mathbf{X})\mathbf{W} - \mathbf{W}^T G(\mathbf{W})\mathbf{W} - M\mathbf{f}^L \otimes \mathbf{1}_N \cdot \mathbf{W}. \quad (15)$$

If the right-hand side of (15) is non-positive, the dynamics of (13) is dissipative. In particular, this would be the case if $\mathbf{f}^L(t) \equiv \mathbf{0}$ since both $G(\mathbf{W})$ and $L(\mathbf{X})$ are positive semi-definite [19].

Remark 4. Clearly, the system would also be dissipative if either $\mathbf{f}^L \otimes \mathbf{1}_N \cdot \mathbf{W} > 0$, for all $t \geq 0$, or if

$$\mathbf{f}^L \otimes \mathbf{1}_N \cdot \mathbf{W} < 0 \quad \text{and} \quad M |\mathbf{f}^L \otimes \mathbf{1}_N \cdot \mathbf{W}| \leq \mathbf{W}^T (L(\mathbf{X}) + G(\mathbf{W})) \mathbf{W}, \quad (16)$$

for all $t \geq 0$. However, it is unclear how to give a rigorous and explicit characterization of the target trajectories that satisfy either of the conditions. To better understand the scenario when $\mathbf{f}^L \otimes \mathbf{1}_N \cdot \mathbf{W} > 0$, observe that $\mathbf{f}^L \otimes \mathbf{1}_N \cdot \mathbf{W} = N \mathbf{f}^L \cdot \bar{\mathbf{w}}$, where $\bar{\mathbf{w}} = \frac{1}{n} \sum_i (\mathbf{v}_i - \mathbf{v}_l)$ is the average deviation of the agents' velocities from the target trajectory. This means that $\mathbf{f}^L \otimes \mathbf{1}_N \cdot \mathbf{W}$ is positive if the angle between \mathbf{f}^L and $\bar{\mathbf{w}}$ is less than $\frac{\pi}{2}$. Informally speaking, this condition can hold when the virtual leader does not steer the group in a direction that is not significantly different from the one the group is currently heading into. In other words, the target trajectory should be sufficiently smooth. However, it is unclear how to quantify such a requirement. For (16) to hold, the dissipation of energy resulting from the action of the ambient force \mathbf{f}_D should, in a way, dominate the influx of energy in the system generated by the acceleration of the virtual leader. In other words, the trajectory is allowed to be less smooth than it should be for $\mathbf{f}^L \otimes \mathbf{1}_N \cdot \mathbf{W} > 0$ to hold, however, its "roughness" should be compensated by the damping effect of the dissipative forces. Still, it is unclear what exact conditions \mathbf{f}^L should satisfy in order for this to be true.

Remark 5. In [31], the moving frame coordinate system chosen to have its origin at the center of mass $(\bar{\mathbf{q}}, \bar{\mathbf{v}}) = \left(\frac{1}{n} \sum_{i=1}^N \mathbf{q}_i, \frac{1}{n} \sum_{i=1}^N \mathbf{v}_i \right)$ of the group. If the generating functions $g(s)$ and $h(s)$ of the self-propulsion forces are constant (so that the forces become linear), in such a coordinate system, the structural dynamics of the group can be decoupled from that of the virtual leader ([31], Lemma 2). As a result, (13) becomes autonomous. Furthermore, the first term in the right-hand side of (15) disappears, so the system is dissipative even when $\mathbf{f}^L(t) \neq \mathbf{0}$. However, since we do not assume that the self-propulsion forces are linear, such an approach is not useful for our purposes. Furthermore, analyzing the structural dynamics of the group relative to the center of mass leaves behind the question of how the center of mass moves relative to the target trajectory (see, e.g., [45]).

For now, suppose that $\mathbf{f}^L(t) \equiv \mathbf{0}$. In this case, if either of $L(\mathbf{X})$ and $G(\mathbf{W})$ is positive definite for all $t \geq 0$, then the system will dissipate energy whenever $\mathbf{W} \neq \mathbf{0}$. In particular, this would be true if $\beta > 0$ and $v_0 = 0$, so that $g(s)$ does not vanish at any point of its domain other than zero and $G(\mathbf{W})$ becomes positive definite. We would refer to such a scenario as *strictly dissipative*. In turn, when either $\beta = 0$ or $v_0 > 0$, $g(s) = 0$ becomes possible for some $s \neq 0$ and all diagonal elements of $G(\mathbf{W})$ can vanish even when $\mathbf{W} \neq \mathbf{0}$. Such a scenario would be referred to as *non-strictly dissipative*.

For both of the above scenarios, $E(\mathbf{X}, \mathbf{W})$ becomes a weak Lyapunov function (see, e.g., [54]) for the autonomous system (13). Fix initial some conditions $(\mathbf{X}(0), \mathbf{W}(0)) = (\mathbf{X}_0, \mathbf{W}_0)$, and let

$$\mathcal{U} = \{(\mathbf{X}, \mathbf{W}) \in \mathbb{R}^{2dN} : E(\mathbf{X}, \mathbf{W}) \leq E(\mathbf{X}_0, \mathbf{W}_0)\},$$

Note that, for any $(\mathbf{X}, \mathbf{W}) \in \mathcal{U}$, we have

$$|\mathbf{W}|^2 \leq \frac{2}{M} E(\mathbf{X}, \mathbf{W}) \leq \frac{2}{M} E(\mathbf{X}_0, \mathbf{W}_0), \quad \Phi(\mathbf{X}) \leq E(\mathbf{X}, \mathbf{W}) \leq E(\mathbf{X}_0, \mathbf{W}_0).$$

and therefore \mathcal{U} , is bounded due to (7). Thus, \mathcal{U} is a compact set that is also positively invariant under the flow generated by (13). By La Salle invariance principle [29], every solution starting in \mathcal{U} would converge to the largest positively invariant subset of the set

$$\mathcal{M} = \{(\mathbf{X}, \mathbf{W}) \in \mathcal{U} : \frac{d}{dt}E(\mathbf{X}(t), \mathbf{W}(t)) = 0\}.$$

Therefore, any solution of (13) converges to the set \mathcal{A} that is a union of orbits satisfying

$$\mathbf{W}^T (L(\mathbf{X}) + G(\mathbf{W})) \mathbf{W} = 0, \quad (17)$$

or, equivalently,

$$B \sum_{(i,j) \in \mathcal{E}(\mathbf{X})} w_D(|\mathbf{x}_{ij}|)(\mathbf{w}_i - \mathbf{w}_j)^2 + \sum_{1 \leq i \leq N, |\mathbf{w}_i| > v_0} g(|\mathbf{w}_i|) |\mathbf{w}_i|^2 = 0, \quad (18)$$

where the first sum is the expansion of the quadratic form $\mathbf{W}^T L(\mathbf{X}) \mathbf{W}$ (see, e.g., [19]).

Let $c(t)$ denote the number of connected components of the proximity graph at time $t \geq 0$, and $N_i(t)$, $i = 1, \dots, c(t)$, be the number of agents in the i -th connected component of the proximity graph at time t . Since g vanishes on $[0, v_0]$, it follows from (18) that, for any solution $(\mathbf{X}^*, \mathbf{W}^*)$ satisfying $(\mathbf{X}^*(t_0), \mathbf{W}^*(t_0)) \in \mathcal{A}$, for some $t_0 \geq 0$, we have

$$\mathbf{W}^*(t) = (\mathbf{w}_1^*(t) \otimes \mathbf{1}_{N_1(t_0)}, \dots, \mathbf{w}_{c(t_0)}^*(t) \otimes \mathbf{1}_{N_{c(t_0)}(t_0)}), \quad (19)$$

where $\mathbf{w}_1^*(t), \dots, \mathbf{w}_{c(t_0)}^*(t) \in \mathbb{R}^d \times [t_0, \infty)$ is such that $|\mathbf{w}_i^*(t)| \leq v_0$ for all $i = 1, \dots, c(t_0)$ and $t \in [t_0, \infty)$. In (19), we assigned consequent indices to agents contained in a given connected component, which could be done without loss of generality. Note that (19) simply means that all agents in a given connected component of the proximity graph will have the same velocity for all $t \geq t_0$.

Thus, for the strictly dissipative case, we arrive at the following result.

Theorem 1. *Suppose $\mathbf{f}^L(t) \equiv \mathbf{0}$. Then, the group of agents exhibits exact proper flocking whenever $\beta > 0$ and $v_0 = 0$.*

Proof. $v_0 = 0$ implies that $\mathbf{W}^*(t) \equiv \mathbf{0}$, and (12) in Definition 1 follows. In turn, (11a) in Definition 1 follows from the fact that \mathcal{U} is bounded for any given initial conditions. \square

Remark 6. In case either $\beta = 0$ or $v_0 > 0$, but the proximity graph can be guaranteed to stay connected at all times, (18) implies that $\mathbf{w}_i = \mathbf{w}_j$, for all $i, j \in \{1, \dots, N\}$. Thus, the system will also exhibit exact flocking, however, it may not be proper.

It is clear that, in the strictly dissipative case, every element of \mathcal{A} is an equilibrium solution. Furthermore, any equilibrium solution of (13) is a positively invariant set satisfying (17), and thus should be contained in \mathcal{A} . Hence, in the strictly dissipative case, \mathcal{A} is precisely the set of equilibrium solutions of (13), and any solution will converge to a flock whose spacial configuration remains *static* relative to the position of the virtual leader. As it is shown in the next section, this might not be the case for the non-strictly dissipative scenario.

4 Wobblers

In this section, our goal is to determine if, in the non-strictly dissipative case, the set \mathcal{A} , given by the union of orbits satisfying (17), may contain non-equilibrium solutions. We will refer to such non-equilibrium solutions as *wobblers*. First, we obtain some sufficient conditions that can guarantee non-existence of wobblers, implying that the qualitative behavior of the system is identical to the one in the strictly dissipative case. Next, we prove the existence of wobblers in special cases and construct them explicitly, demonstrating that the asymptotic flocks might not be static relative to the position of the virtual leader.

Suppose that $(\mathbf{X}^*, \mathbf{W}^*)$ is such that $(\mathbf{X}^*(t_0), \mathbf{W}^*(t_0)) \in \mathcal{A}$ for some $t_0 \geq 0$. For simplicity, consider the case when the proximity graph is connected at t_0 , so that, for all $t \geq t_0$,

$$\mathbf{W}(t) = (\mathbf{w}^*(t), \mathbf{w}^*(t), \dots, \mathbf{w}^*(t)) \quad (20)$$

for some $\mathbf{w}^*(t) \in \mathbb{R}^d \times [t_0, \infty)$ satisfying

$$|\mathbf{w}^*(t)| \leq v_0 \quad (21)$$

In case $c(t_0) > 1$, the forthcoming analysis could simply be applied to each of the individual connected components. The trajectory $(\mathbf{X}^*, \mathbf{W}^*)$ satisfying (20) solves

$$\begin{aligned} \dot{\mathbf{X}}^* &= \mathbf{W}^*, \\ \dot{\mathbf{w}}^* &= \mathbf{f}_i^C + \mathbf{u}(\mathbf{x}_i^*), \quad i = 1, 2, \dots, N, \end{aligned} \quad (22)$$

with $\mathbf{u}(\mathbf{x}_i^*) = -h(\mathbf{x}_i^*)\mathbf{x}_i^*$. Let $\mathbf{x}_i^0 = \mathbf{x}_i(t_0)$, $i = 1, \dots, N$, and write

$$\mathbf{x}_i^*(t) = \mathbf{x}_i^0 + \mathbf{x}^*(t), \quad (23)$$

where

$$\mathbf{x}^*(t) = \int_0^t \mathbf{w}^*(\tau) d\tau.$$

Since conservative forces \mathbf{f}_i^C are functions of relative positions, (23) implies that the differences

$$\mathbf{u}(\mathbf{x}_i^*) - \mathbf{u}(\mathbf{x}_j^*)$$

are independent of t . Therefore,

$$\mathbf{u}(\mathbf{x}_i^0 + \mathbf{x}^*(t)) - \mathbf{u}(\mathbf{x}_j^0 + \mathbf{x}^*(t)) = \mathbf{u}(\mathbf{x}_i^0) - \mathbf{u}(\mathbf{x}_j^0) \quad (24)$$

for all $t \in [0, \infty)$. Equation (24) implies existence of $\mathbf{d}(t) : [0, \infty) \rightarrow \mathbb{R}^d$ such that

$$\mathbf{u}(\mathbf{x}_i^0 + \mathbf{x}^*(t)) = \mathbf{d}(t) + \mathbf{u}(\mathbf{x}_i^0) \quad (25)$$

for all $i = 1, 2, \dots, N$.

We further impose the following natural requirements. First, we assume that no agents can have the same initial position

$$\mathbf{x}_i^0 \neq \mathbf{x}_j^0 \quad \text{if } i \neq j \quad (26)$$

for $i, j = 1, 2, \dots, N$. We also require the group to stay cohesive, so that acceptable solutions of (22) should satisfy

$$|\mathbf{x}_j^0 + \mathbf{x}^*(t)| \leq R \quad (27)$$

for some $R > 0$ and all $t \in [t_0, \infty)$ and $j = 1, 2, \dots, N$. Finally, we assume that \mathbf{w}^* does not vanish on intervals:

$$\forall t_1, t_2 \in \mathbb{R}, \quad t_0 \leq t_1 < t_2 \Rightarrow \mathbf{w}^*(t) \not\equiv 0 \text{ on } (t_1, t_2). \quad (28)$$

If there exist $t_1, t_2 \in \mathbb{R}, t_0 \leq t_1 < t_2$, such that $\mathbf{w}^*(t) \equiv 0$ on (t_1, t_2) , it follows that $\mathbf{w}^*(t) \equiv 0$ on (t_1, ∞) making $(\mathbf{X}^*, \mathbf{W}^*)$ an equilibrium solution which is not of our interest in this section.

Definition 2. *A wobbler is a solution of (22) satisfying (21), (26), (27), and (28).*

4.1 Non-linear case: non-existence

First, suppose that the generating function $h(s)$ is non-linear, i.e., either that $r_0 > 0$ or that $k(s)$ is not a multiple of s . In this case, we can eliminate the existence of wobblers for a certain class of functions $k(s)$ when the group consists of *more than two agents*. To do so, we would need a few auxiliary results.

Lemma 1. *Let $f : \mathbb{R} \rightarrow \mathbb{R}_{\geq 0}$ be continuous and $S = \{x \in \mathbb{R} \mid f(x) = 0\}$. For any open $I \subseteq \mathbb{R}$, if $I \cap S$ is dense in I , then $f(x) = 0$ on I .*

Proof. See Appendix A. □

Note that it follows from (6) that $\mathbf{u}(x)$ is one-to-one outside of the ball $B(\mathbf{0}, r_0)$ since $k(s)$ is strictly increasing.

Proposition 1. *Suppose $(\mathbf{X}^*, \mathbf{W}^*)$ is a wobbler. Then there exists an open interval $I \subseteq (t_0, \infty)$ such that*

- (i) $|\mathbf{x}_i^*(t)| > r_0$ on I , for all $i = 1, \dots, N$;
- (ii) $\mathbf{d}(t)$ cannot be constant on any open subinterval of I .

Proof. Define

$$\mathcal{I}_-(t) = \{i \mid |\mathbf{x}_i^*(t)| < r_0\}, \quad \mathcal{I}_0(t) = \{i \mid |\mathbf{x}_i^*(t)| = r_0\}, \quad \mathcal{I}_+(t) = \{i \mid |\mathbf{x}_i^*(t)| > r_0\},$$

for all $t \geq t_0$

Suppose (i) is false and let $I \subseteq (t_0, \infty)$ be open. Then there exists $\tau \in I$ such that $\mathcal{I}_0(\tau) \cup \mathcal{I}_-(\tau)$ is non-empty. Suppose $\mathcal{I}_+(\tau)$ is also non-empty. By continuity of \mathbf{x}^* , $i \in \mathcal{I}_-(\tau) \cup \mathcal{I}_+(\tau)$ implies that there exists $\delta_i > 0$ such that either $i \in \mathcal{I}_-(t)$, for all $t \in (\tau - \delta_i, \tau + \delta_i)$, or $i \in \mathcal{I}_+(t)$, for all $t \in (\tau - \delta_i, \tau + \delta_i)$. Thus

$$\mathcal{I}_-(t) = \mathcal{I}_-(\tau), \quad \mathcal{I}_+(t) = \mathcal{I}_+(\tau), \quad (29)$$

on $\tilde{I} = (\tau - \delta, \tau + \delta)$, where $\delta = \min_{i \in \mathcal{I}_-(\tau) \cup \mathcal{I}_+(\tau)} \delta_i$. Then, for any $i \in \mathcal{I}_-(\tau)$ and for any $j \in \mathcal{I}_+(\tau)$, subtracting the j -th equation from the i -th equation in (22) yields

$$\mathbf{u}(\mathbf{x}_j^*(t)) = \mathbf{f}_i^C - \mathbf{f}_j^C,$$

for all $t \in \tilde{I}$. (23) implies that $\mathbf{x}_i(t) - \mathbf{x}_j(t) = \mathbf{x}_i^0 - \mathbf{x}_j^0$, for all $i, j \in \{1, \dots, N\}$ and for all $t \geq t_0$, and thus $\mathbf{f}_i^C - \mathbf{f}_j^C$ is constant. Therefore $\mathbf{u}(\mathbf{x}_j^*(t))$ is constant on \tilde{I} , and so is $\mathbf{x}_j^*(t)$ since \mathbf{u} is one-to-one. Then $\mathbf{w}^*(t) = 0$ on \tilde{I} , which contradicts the definition of a wobbler, and therefore $\mathcal{I}_-(\tau)$ must be empty. An analogous argument could be used to show that there is no open interval containing τ such that $i \in \mathcal{I}_0(t)$ on it, for some $i \in \mathcal{I}_0(\tau)$, unless $\mathcal{I}_+(\tau)$ is empty.

Let $i_1 \in \mathcal{I}_0(\tau)$. If the set $S_1 = \{t \in \tilde{I} \mid i_1 \in \mathcal{I}_0(t)\}$ is dense in \tilde{I} , then, by Lemma 1, $i_1 \in \mathcal{I}_0(t)$ on \tilde{I} which is a contradiction. Therefore, there exists an open interval $\tilde{I}_1 \subseteq \tilde{I}$ such that $i_1 \in \mathcal{I}_0(t)$, for all $t \in \tilde{I}_1$. Similarly, if $i_2 \in \mathcal{I}_0(\tau) \setminus \{i_1\}$, then there exists an open interval $\tilde{I}_2 \subseteq \tilde{I}_1$, such that $i_2 \in \mathcal{I}_0(t)$, for all $t \in \tilde{I}_2$. Applying the above procedure for all $i \in \mathcal{I}_0(\tau) \setminus \{i_1, i_2\}$, one gets that exists an open interval $\tilde{I}_N \subseteq \dots \subseteq \tilde{I}_1$ such that $\mathcal{I}_+(t) = \{1, \dots, N\}$, for all $t \in \tilde{I}_N$, which is a contradiction. Thus $\mathcal{I}_+(\tau)$ is empty unless $\mathcal{I}_0(\tau) \cup \mathcal{I}_-(\tau)$ is empty. In fact, since I and τ were chosen arbitrarily, we showed that, for any $t \geq t_0$, either $\mathcal{I}_0(t) \cup \mathcal{I}_-(t)$ or $\mathcal{I}_+(t)$ must be empty.

Let $t_1, t_2 \geq t_0$ be such that $[t_1, t_2]$ is the maximal interval containing τ on which $\mathcal{I}_+(t)$ is empty. Clearly, $t_1 < t_2$. Adding N equations in (22), due to pairwise symmetry of the ambient conservative force, we get that $\mathbf{w}^*(t) = 0$ on $[t_1, t_2]$. Hence

$$\mathbf{x}_i^*(t) = \mathbf{x}_i^*(t_1) + \mathbf{C}(t - t_1), \quad i = 1, \dots, N, \quad (30)$$

for all $t \in [t_1, t_2]$ and some constant $\mathbf{C} \in \mathbb{R}^d$, $\mathbf{C} \neq \mathbf{0}$. Since $\mathbf{x}_i^*(t)$ defined by (30) is unbounded as $t \rightarrow \infty$, t_2 must be finite. Therefore, there exists $t_3 > t_2$ such that $\mathcal{I}_+(t_3)$ is non-empty. Thus (i) has to be true.

Now, suppose (ii) is false and let $I \subseteq (t_0, \infty)$ be open and such that (i) holds on it, but $\mathbf{d}(t) = \mathbf{d}_0$, for all $t \in I$ and some constant $\mathbf{d}_0 \in \mathbb{R}^d$. It follows from (25) that

$$\mathbf{u}(\mathbf{x}_i^*(t_1)) = \mathbf{u}(\mathbf{x}_i^*(t_2)),$$

for all $t_1, t_2 \in I$ and for all $i = 1, \dots, N$. Since \mathbf{u} is one-to-one, $\mathbf{x}_i^*(t)$ is constant on I , and hence $\mathbf{w}^*(t) = 0$ on I . This contradicts the definition of a wobbler. Thus (ii) must be true. \square

Remark 7. If the control parameter α is set to 0 and the position alignment force is disabled, we get that $\mathbf{d}(t) \equiv \mathbf{0}$. By part (ii) of Proposition 1, this contradicts the existence of wobblers. Thus, the presence of the position alignment force is a necessary condition for wobblers to exist.

Lemma 2. Suppose $h(s)$ is twice differentiable and that $h(s)$, $sh'(s)$ and $\frac{s(h'(s))^2}{2h'(s) + (sh'(s))'}$ are strictly increasing on (r_0, ∞) . Then, for any $a, b \in \mathbb{R}$, the equation

$$[h(s) - a][h(s) - a + sh'(s)] = -b^2 \quad (31)$$

has at most two solutions.

Proof. Define

$$F(s) = [h(s) - a] [h(s) - a + sh'(s)], \quad s > r_0,$$

and let $s_1, s_2 > r_0$ be such that $h(s_1) = a$ and $h(s_2) + s_2 h'(s_2) = a$, so that $F(s_1) = F(s_2) = 0$. Since both $h(s)$ and $sh'(s)$ are increasing, we have that $s_1 < s_2$, and that $F(s) < 0$ on the interval (s_1, s_2) , and $F(s) > 0$ outside of this interval. Thus, if a solution of (31) exists, it has to belong to the interval $[s_1, s_2]$.

If $b = 0$, then s_1 and s_2 are the solutions of (31), and no other solutions exist since $h(s)$ and $sh'(s)$ are increasing. Therefore suppose that $b \neq 0$. By Rolle's theorem, F has a critical point s_c on (s_1, s_2) . We have

$$0 = F'(s_c) = h'(s_c) [h(s_c) - a + s_c h'(s_c)] + [h(s_c) - a] [h'(s_c) + (s_c h'(s_c))'],$$

which yields

$$h(s_c) - a = -\frac{s_c (h'(s_c))^2}{2h'(s_c) + (s_c h'(s_c))'}. \quad (32)$$

By assumptions of the lemma, the LHS is increasing and the RHS is decreasing, and so s_c is the unique solution of (32). Thus, F has only one critical point on (s_1, s_2) and $F(s) = -b^2$ has at most two solutions on (s_1, s_2) . This completes the proof. \square

We now prove the main result of this section.

Theorem 2. *Suppose $h(s)$ satisfy the assumptions of Lemma 2 and that $N > 2$. Then wobblers do not exist.*

Proof. Suppose $(\mathbf{X}^*, \mathbf{W}^*)$ is a wobbler. By Proposition 1, there exist $t_1, t_2 \in \mathbb{R}$, $t_0 \leq t_1 < t_2$, such that $\mathbf{d}(t_1) \neq \mathbf{d}(t_2)$ and that $|\mathbf{x}_i^*(t)| \in B_i \subseteq \mathbb{R}^d$, where B_i is an open ball lying outside of the ball $B(0, r_0)$, for all $t \in [t_1, t_2]$ and for all $i = 1, \dots, N$.

Fix $i \in \{1, \dots, N\}$ and let $\mathbf{y}_1 = \mathbf{x}_i^*(t_1)$, $\mathbf{y}_2 = \mathbf{x}_i^*(t_2)$, $\mathbf{y}^* = \mathbf{y}_2 - \mathbf{y}_1$, $\mathbf{d}^* = \mathbf{d}(t_2) - \mathbf{d}(t_1)$. Using a first-degree Taylor expansion of \mathbf{u} at \mathbf{y}_1 , we can write (24) as

$$\frac{1}{\beta} \mathbf{d}^* = \mathbf{u}(\mathbf{y}_2) - \mathbf{u}(\mathbf{y}_1) = \nabla \mathbf{u}(\mathbf{y}) \mathbf{y}^* = -|\mathbf{y}| h'(|\mathbf{y}|) \left(\frac{\mathbf{y}}{|\mathbf{y}|} \otimes \frac{\mathbf{y}}{|\mathbf{y}|} \right) \mathbf{y}^* - h(|\mathbf{y}|) \mathbf{y}^*, \quad (33)$$

where \mathbf{y} belongs to the line segment connecting \mathbf{y}_1 and \mathbf{y}_2 , so that $\mathbf{y} \in B_i$ and $\mathbf{y} \neq \mathbf{0}$. Write (33) as

$$|\mathbf{y}| h'(|\mathbf{y}|) \left(\frac{\mathbf{y}}{|\mathbf{y}|} \cdot \mathbf{y}^* \right) \frac{\mathbf{y}}{|\mathbf{y}|} = \mathbf{p}, \quad (34)$$

where $\mathbf{p} = -\frac{1}{\beta} \mathbf{d}^* - h(|\mathbf{y}|) \mathbf{y}^*$. Since $\frac{\mathbf{y}}{|\mathbf{y}|}$ is a unit vector that is collinear with \mathbf{p} , we can write

$$|\mathbf{y}| h'(|\mathbf{y}|) \left(\frac{\mathbf{p}}{|\mathbf{p}|} \cdot \mathbf{y}^* \right) \frac{\mathbf{p}}{|\mathbf{p}|} = \mathbf{p}. \quad (35)$$

Note that $\mathbf{y}^* \neq \mathbf{0}$ since $\mathbf{d}^* \neq \mathbf{0}$ and \mathbf{u} is one-to-one. Also, $h'(s) > 0$ whenever $s > r_0$ by the assumption of the theorem. Thus (35) is equivalent to

$$|\mathbf{y}| h'(|\mathbf{y}|) (\mathbf{p} \cdot \mathbf{y}^*) = |\mathbf{p}|^2, \quad (36)$$

for all $\mathbf{p} \neq \mathbf{0}$.

Suppose $\mathbf{p} = \mathbf{0}$, so that $\frac{1}{\beta} \mathbf{d}^* = -h(|\mathbf{y}|) \mathbf{y}^*$. Then (24) yields

$$-h(|\mathbf{y}|) \mathbf{y}^* = -h(|\mathbf{y}_1 + \mathbf{y}^*|)(\mathbf{y}_1 + \mathbf{y}^*) + h(|\mathbf{y}_1|) \mathbf{y}_1.$$

Rearranging terms, we get

$$[h(|\mathbf{y}_1 + \mathbf{y}^*|) - h(|\mathbf{y}_1|)] \mathbf{y}_1 + [h(|\mathbf{y}_1 + \mathbf{y}^*|) - h(|\mathbf{y}|)] \mathbf{y}^* = \mathbf{0}. \quad (37)$$

If \mathbf{y}_1 is collinear with \mathbf{y}^* , then so are $\mathbf{y}_2 = \mathbf{y}_1 + \mathbf{y}^*$ and \mathbf{y} . However, it follows from (34) that $\mathbf{y} \cdot \mathbf{y}^* = \mathbf{0}$, and thus \mathbf{y}_1 and \mathbf{y}^* have to be linearly independent. Then (37) implies that

$$h(|\mathbf{y}_1 + \mathbf{y}^*|) - h(|\mathbf{y}_1|) = h(|\mathbf{y}_1 + \mathbf{y}^*|) - h(|\mathbf{y}|) = 0,$$

and hence

$$|\mathbf{y}_1 + \mathbf{y}^*| = |\mathbf{y}_1| = |\mathbf{y}|,$$

which is not possible since \mathbf{y} belongs to the line segment connecting \mathbf{y}_1 and $\mathbf{y}_1 + \mathbf{y}^*$. Therefore $\mathbf{p} \neq \mathbf{0}$.

Let \mathbf{y}^\perp be such that $\mathbf{y}^* \cdot \mathbf{y}^\perp = 0$ and $\frac{1}{\beta} \mathbf{d}^* = -a\mathbf{y}^* - \mathbf{y}^\perp$, for some $a \in \mathbb{R}$. Then (36) could be written as

$$sh'(s) (a\mathbf{y}^* + \mathbf{y}^\perp - h(s)\mathbf{y}^*) \cdot \mathbf{y}^* = |a\mathbf{y}^* + \mathbf{y}^\perp - h(s)\mathbf{y}^*|^2,$$

from which we get

$$|\mathbf{y}| h'(|\mathbf{y}|) [h(|\mathbf{y}|) - a] |\mathbf{y}^*|^2 = [h(|\mathbf{y}|) - a]^2 |\mathbf{y}^*|^2 + |\mathbf{y}^\perp|^2,$$

and so

$$[h(|\mathbf{y}|) - a]^2 + |\mathbf{y}| h'(|\mathbf{y}|) [h(|\mathbf{y}|) - a] = -\frac{|\mathbf{y}^\perp|^2}{|\mathbf{y}^*|^2}. \quad (38)$$

By Lemma 2, (38) has at most two distinct solutions for $|\mathbf{y}|$. Furthermore, since \mathbf{y} and \mathbf{p} are collinear and \mathbf{p} is completely determined by $|\mathbf{y}|$, so is \mathbf{y} . Thus (35) has at most two solutions for \mathbf{y} . Finally, since (35) depends on i only through \mathbf{y} , it follows that $(\mathbf{X}^*, \mathbf{W}^*)$ does not exist provided $N > 2$. \square

As it could be seen from the following example, the assumptions of Lemma 2 are easy to satisfy.

Example 1. Suppose $k_1(s) = s^{\gamma+1}$, $\gamma > 0$, $s \geq r_1$, for some $r_1 > r_0$, then

$$h_1(s) = \frac{k_1(s)}{s} = s^\gamma, \quad sh'_1(s) = \gamma s^\gamma, \quad \frac{s(h'_1(s))^2}{2h'_1(s) + (sh'_1(s))'} = \frac{\gamma}{\gamma + 2} s^\gamma,$$

are all increasing on (r_1, ∞) . If one puts $h_2(s) = se^s$, $s \geq r_2$, for some $r_2 > r_0$, then

$$h_2(s) = \frac{k_2(s)}{s} = e^s, \quad sh'_2(s) = se^s, \quad \frac{s(h'_2(s))^2}{2h'_2(s) + (sh'_2(s))'} = \frac{s}{s + 3} e^s.$$

One could verify that the above functions are increasing on (r_2, ∞) by computing the corresponding derivatives. Similarly, if $k_3(s) = s \ln(s+1)$, $s \geq r_3$, for some $r_3 > r_0$, then

$$h_3(s) = \frac{k_3(s)}{s} = \ln(s+1), \quad sh'_3(s) = \frac{s}{s+1}, \quad \frac{s(h'_3(s))^2}{2h'_3(s) + (sh'_3(s))'} = \frac{s}{2s+3},$$

are increasing on (r_3, ∞) . Thus, it is easy to guarantee non-existence of wobblers for a large class of non-linear position alignment forces.

4.2 Linear case: existence

Now, suppose that $\alpha \neq 0$, $r_0 = 0$ and $k(s) = s$, so that

$$\mathbf{u}(\mathbf{x}) = -\alpha \mathbf{x}$$

is linear. Equations (22) could be written as

$$\ddot{\mathbf{x}}^* + \alpha \mathbf{x}^* = \mathbf{f}_i^C - \alpha \mathbf{x}_i^0, \quad i = 1, \dots, N. \quad (39)$$

Since the left-hand side does not depend on the index i , and the right-hand side does not depend on t , the right-hand side is a constant vector which we denote by \mathbf{f}^0 . We assume that the equations of motion are supplemented with the initial conditions

$$\mathbf{x}^*(t_0) = \mathbf{0}, \quad \dot{\mathbf{x}}^*(t_0) = \mathbf{w}^*(0). \quad (40)$$

Solving the characteristic equation for (39) yields the fundamental set of solutions $\cos \mu t, \sin \mu t$, where $\mu = \alpha^{1/2}$. The solution of the IVP (39), (40) is

$$\mathbf{x}^*(t) = \mathbf{a} \cos(\mu t) + \mathbf{b} \sin(\mu t) + \alpha^{-1} \mathbf{f}^0, \quad (41)$$

where

$$\mathbf{a} = -\alpha^{-1} \cos \mu t_0 \mathbf{f}^0 - \mu^{-1} \sin \mu t_0 \mathbf{w}_0^*, \quad (42)$$

$$\mathbf{b} = \mu^{-1} \cos \mu t_0 \mathbf{w}_0^* - m^{-1} \sin \mu t_0 \mathbf{f}^0 \quad (43)$$

Equations (41)-(43) describe a periodic translation of the initial array $\mathbf{X}_0^* = (\mathbf{x}_1^0, \dots, \mathbf{x}_N^0)$. The dependence of this array on the parameter \mathbf{f}_0 , is prescribed by solving the quasi-equilibrium equations

$$\mathbf{f}_i^C(\mathbf{X}_0^*) + \mathbf{u}(\mathbf{x}_i^0) = \mathbf{f}^0.$$

for any \mathbf{f}^0 that would yield $\mathbf{X}^*, \mathbf{W}^*$ compatible with (21) and (27).

Example 2. Suppose that $t_0 = 0$ and consider an equilibrium solution ($\mathbf{f}^0 = \mathbf{0}$) as the initial array. Then for each admissible $\mathbf{w}^*(0) \neq \mathbf{0}$, the initial array undergoes a rigid periodic translation

$$\mathbf{x}_i^*(t) = \mathbf{x}_i^0 + \mu^{-1} \sin(\mu t) \mathbf{w}^*(0), \quad i = 1, 2, \dots, N. \quad (44)$$

The inequalities (21) and (27) impose restrictions on \mathbf{x}_i^0 , μ and $\mathbf{w}^*(0)$. In particular,

$$|\mathbf{x}_i^0| \leq R,$$

and

$$|\mathbf{x}_i^0 + \mu^{-1}\mathbf{w}^*(0)| \leq R,$$

where $\mathbf{w}^*(0)$ must also satisfy (21).

5 Non-dissipative dynamics

The assumption $\mathbf{f}^L(t) \equiv \mathbf{0}$, used in the previous sections, may be too restrictive for practical applications. Therefore, in this section, we turn our attention to the case when $\mathbf{f}^L(t) \not\equiv \mathbf{0}$. In this case, the Laypunov-like argument used earlier does not apply since the total mechanical energy (14) cannot be guaranteed to be a non-increasing function. By means of an alternative argument, working under the assumption that the self-propulsion forces are bounded perturbations of linear ones, we first show that the solutions of (1) are bounded and the system has a global attractor. Thus, the system exhibits proper flocking. Next, we show that for some special configurations of the tunable parameters, the flocking becomes exact. We then consider the structural dynamics of the group and show that the velocities of the agents converge to the velocity of the center of mass at an exponential rate under some mild additional assumptions on the non-linearities of the self-propulsion forces. Thus, the system exhibits exact flocking. Finally, we show that the deviation of the trajectory of the center of mass from that of the virtual leader is bounded.

5.1 Boundedness of solutions

The first assumption we make is that the acceleration of the virtual leader is bounded, which is natural to expect in any practical application.

Assumption 1. *There exists $C_l \geq 0$ such that $|\mathbf{f}^L(t)| \leq C_l$, for all $t \geq 0$.*

In addition, we restrict our attention to the self-propulsion forces that are bounded perturbations of the linear ones.

Definition 3. *A function $\mathbf{f} : \mathbb{R}^d \rightarrow \mathbb{R}^d$ is **approximately linear** if there exist real constants $K \neq 0$ and $C > 0$ such that*

$$|\mathbf{f}(\mathbf{y}) - K\mathbf{y}| \leq C$$

for all $\mathbf{y} \in \mathbb{R}^d$ and $t \in [0, \infty)$.

Assumption 2. *The position alignment force \mathbf{u}^P and the velocity alignment force \mathbf{u}^V are approximately linear with constants $-K_p$, C_p and $-K_v$, C_v , respectively, where $K_p, K_v > 0$.*

Note that, in real-world applications, the asymptotic behavior of the self-propulsion forces is irrelevant, and hence the class of approximately linear functions contains a wide range of non-linear control protocols that might be of practical interest.

Let

$$\delta \mathbf{u}^P(\mathbf{y}) = \mathbf{u}^P(\mathbf{y}) + K_p \mathbf{y}, \quad \mathbf{y} \in \mathbb{R}^d,$$

and

$$\delta \mathbf{u}^V(\mathbf{y}) = \mathbf{u}^V(\mathbf{y}) + K_v \mathbf{y}, \quad \mathbf{y} \in \mathbb{R}^d,$$

denote the non-linear parts of the position alignment and the velocity alignment self-propulsion forces, respectively. Write (13) as

$$\begin{aligned} \dot{\mathbf{X}} &= \mathbf{W}, \\ M \dot{\mathbf{W}} &= -\nabla_{\mathbf{X}} U(\mathbf{X}) - L(\mathbf{X}) \mathbf{W} - K_p \mathbf{X} - K_v \mathbf{W} + \mathbf{F}(t), \end{aligned} \tag{45}$$

where

$$\mathbf{F}(t) = \delta \mathbf{u}^P(\mathbf{X}) + \delta \mathbf{u}^V(\mathbf{W}) - M \mathbf{f}^L \otimes \mathbf{1}_N,$$

and

$$\delta \mathbf{u}^P(\mathbf{X}) = \text{diag}(\delta \mathbf{u}^P(\mathbf{x}_1), \dots, \delta \mathbf{u}^P(\mathbf{x}_N)), \quad \delta \mathbf{u}^V(\mathbf{W}) = \text{diag}(\delta \mathbf{u}^V(\mathbf{v}_1), \dots, \delta \mathbf{u}^V(\mathbf{v}_N)).$$

Note that it follows from Assumptions 1 and 2 that

$$|\mathbf{F}(t)| \leq C_1, \tag{46}$$

for all $t \geq 0$, where

$$C_1 = N^{\frac{1}{2}}(C_p + C_v + MC_l).$$

Consider the following reduced system

$$\begin{aligned} \dot{\mathbf{X}} &= \mathbf{W}, \\ M \dot{\mathbf{W}} &= -\nabla_{\mathbf{X}} U(\mathbf{X}) - L(\mathbf{X}) \mathbf{W} - K_p \mathbf{X} - K_v \mathbf{W}. \end{aligned} \tag{47}$$

We first prove that the velocities of the reduced system (47) decay exponentially.

Lemma 3. *Let $(\mathbf{X}(t), \mathbf{W}(t))$ be a solution of the reduced system (47). Then for any $t_0 \geq 0$,*

$$|\mathbf{W}(t)| \leq |\mathbf{W}(t_0)| e^{-\frac{K_v}{M}(t-t_0)},$$

for all $t \geq t_0$.

Proof. Let

$$E_r(\mathbf{X}, \mathbf{W}) = \frac{1}{2} M |\mathbf{W}|^2 + U(\mathbf{X}) + \frac{1}{2} K_p |\mathbf{X}|^2. \tag{48}$$

Multiplying both sides of the second equation in (47) by \mathbf{W} yields

$$\frac{d}{dt} E_r(\mathbf{X}(t), \mathbf{W}(t)) = -\mathbf{W}^T L(\mathbf{X}) \mathbf{W} - K_v |\mathbf{W}|^2 \leq -K_v |\mathbf{W}|^2, \tag{49}$$

since $L(\mathbf{X})$ is positive semi-definite.

Let $t_0 \geq 0$. Integrating both side of (49), we get

$$E_r(\mathbf{X}(t), \mathbf{W}(t)) \leq -K_v \int_{t_0}^t |\mathbf{W}(\tau)|^2 d\tau + E_r(t_0),$$

where $E_r(t_0) = E(\mathbf{X}(t_0), \mathbf{W}(t_0))$. Hence

$$|\mathbf{W}(t)|^2 \leq -\frac{2K_v}{M} \int_{t_0}^t |\mathbf{W}(\tau)|^2 d\tau + \frac{2E_r(t_0)}{M}. \quad (50)$$

Let $\Lambda(t) = \int_{t_0}^t |\mathbf{W}(\tau)|^2 d\tau$. Multiplying both sides of (50) by $e^{\frac{2K_v}{M}(t-t_0)}$ yields

$$\frac{d}{dt} \left(e^{\frac{2K_v}{M}(t-t_0)} \Lambda(t) \right) \leq \frac{2E_r(t_0)}{M} e^{\frac{2K_v}{M}(t-t_0)}. \quad (51)$$

Integrating (51), we get

$$e^{\frac{2K_v}{M}(t-t_0)} \Lambda(t) \leq \Lambda(t_0) + \frac{E_r(t_0)}{K_v} \left(e^{\frac{2K_v}{M}(t-t_0)} - 1 \right),$$

and therefore

$$\int_{t_0}^t |\mathbf{W}(\tau)|^2 d\tau \leq \frac{E_r(t_0)}{K_v} \left(1 - e^{-\frac{2K_v}{M}(t-t_0)} \right), \quad (52)$$

since $\Lambda(t_0) = 0$. Differentiating (52) yields

$$\begin{aligned} |\mathbf{W}(t)|^2 &\leq \frac{2E_r(t_0)}{M} e^{-\frac{2K_v}{M}(t-t_0)} \\ &\leq E_r(t_0) \left(\frac{1}{2} M |\mathbf{W}(t_0)|^2 \right)^{-1} |\mathbf{W}(t_0)|^2 e^{-\frac{2K_v}{M}(t-t_0)} \\ &\leq |\mathbf{W}(t_0)|^2 e^{-\frac{2K_v}{M}(t-t_0)}, \end{aligned}$$

and the result follows. \square

Now, observe that analogously to the ambient dissipative term $-L(\mathbf{W})\mathbf{W}$, the ambient conservative term $-\nabla_{\mathbf{X}}U(\mathbf{X})$ in (45) and (47) could be written as $L_C(\mathbf{X})\mathbf{X}$, with $L_C(\mathbf{X}) = \mathcal{L}_C(\mathbf{X}) \otimes I_d$, where $\mathcal{L}_C(\mathbf{X})$ is the Laplacian matrix of the position-dependent undirected weighted graph $\mathcal{G}_C(\mathbf{X}) = (\mathcal{A}, \mathcal{E}_C(\mathbf{X}), \sigma_C)$, with $\mathcal{A} = \{1, \dots, N\}$, $\mathcal{E}_C(\mathbf{X}) = \{(i, j) \in \mathcal{A} \times \mathcal{A} : |\mathbf{x}_{ij}| \leq r_C\}$, and $\sigma_C(i, j) = A w_C(|\mathbf{x}_{ij}|)$. This means that (47) could be viewed as a linear non-autonomous system, and (45) could be viewed as its non-homogeneous counterpart. This observation along with Lemma 3 allows us to show that the velocities of the full system (45) are bounded.

Lemma 4. *Let $(\mathbf{X}(t), \mathbf{W}(t))$ be a solution of the full system (45). Suppose Assumptions 1 and 2 hold. Then, for any $\varepsilon_0 > 0$, there exists $t_0 = t_0(\mathbf{W}(0), \varepsilon_0) \geq 0$ such that*

$$|\mathbf{W}(t)| \leq \varepsilon_0 + \frac{C_1}{K_v},$$

for all $t \geq t_0$.

Proof. Let $\Psi(t, s)$, $t \geq s \geq 0$ be the transition matrix of the linear system (47). By the variation of constants formula, the solution of (45) is given by

$$(\mathbf{X}(t), \mathbf{W}(t)) = \Psi(t, 0)(\mathbf{X}(0), \mathbf{W}(0)) + \int_0^t \Psi(t, \tau)(\mathbf{0}, M^{-1}\mathbf{F}(\tau))d\tau, \quad (53)$$

Let $\Psi_{\mathbf{W}}(t, s)$ be the last Nd rows of be the matrix $\Psi(t, s)$, i.e., $\Psi_{\mathbf{W}}(t, s)$ is such that the velocity components of the solution of (47) are given by $\Psi_{\mathbf{W}}(t, s)(\mathbf{X}(s), \mathbf{W}(s))$. Then, it follows from (46), (53), and Lemma (3) that

$$\begin{aligned} |\mathbf{W}(t)| &\leq |\Psi_{\mathbf{W}}(t, 0)(\mathbf{X}(0), \mathbf{W}(0))| + \left| \int_0^t \Psi_{\mathbf{W}}(t, \tau)_{\mathbf{W}}(\mathbf{0}, M^{-1}\mathbf{F}(\tau))d\tau \right| \\ &\leq |\mathbf{W}(0)| e^{-\frac{K_v}{M}t} + \frac{1}{M} \int_0^t |\mathbf{F}(\tau)| e^{-\frac{K_v}{M}\tau} d\tau \\ &= \left(|\mathbf{W}(0)| - \frac{C_1}{K_v} \right) e^{-\frac{K_v}{M}t} + \frac{C_1}{K_v} \end{aligned}$$

Since $K_v > 0$, the result follows. \square

Equipped with the above lemma we are ready to prove that the solutions of the full system (45) are bounded.

Theorem 3. *Let $(\mathbf{X}(t), \mathbf{W}(t))$ be a solution of (45). Suppose that Assumptions 1 and 2 hold, and that $\tilde{K}_v^2 - 4\tilde{K}_p \neq 0$, where $\tilde{K}_p = M^{-1}K_p$, $\tilde{K}_v = M^{-1}K_v$. Then, for any $i = 1, \dots, N$, and for any $\varepsilon_1 > 0$, there exists $t_1 = t_1(\mathbf{x}_i(0), \mathbf{w}_i(0), \varepsilon_1) \geq 0$ such that*

$$(i) \quad |\mathbf{x}_i(t)| \leq \varepsilon_1 + \frac{2\tilde{K}_v}{\tilde{K}_p \sqrt{|\tilde{K}_v^2 - 4\tilde{K}_p|}} C_2;$$

$$(ii) \quad |\mathbf{w}_i(t)| \leq \varepsilon_1 + \frac{2}{\sqrt{|\tilde{K}_v^2 - 4\tilde{K}_p|}} C_2;$$

for all $t \geq t_1$, where

$$C_2 = \frac{1}{M} \left[(N-1)^{\frac{1}{2}} Ar_C + (N^2 - N)^{\frac{1}{2}} \frac{BC_1}{K_v} + N^{-\frac{1}{2}} C_1 \right].$$

Proof. Write (45) as

$$\begin{aligned} \dot{\mathbf{x}}_i &= \mathbf{w}_i, \\ M\dot{\mathbf{w}}_i &= -K_p \mathbf{x}_i - K_v \mathbf{w}_i + \mathbf{H}_i(t), \quad i = 1, \dots, N, \end{aligned} \quad (54)$$

where

$$\mathbf{H}_i(t) = \mathbf{f}_i^C + \mathbf{f}_i^D + \mathbf{F}_i(t).$$

Let $\varepsilon_0 > 0$. It follows from Lemma 4 that there exists $t_0 = t_0(\mathbf{W}(0), \varepsilon_0) \geq 0$ such that

$$|\mathbf{H}_i(t)| = \left| A \sum_{j \neq i} w_C(|\mathbf{x}_{ij}|) \mathbf{x}_{ij} - B \sum_{j \neq i} w_D(|\mathbf{x}_{ij}|) \mathbf{w}_{ij} + \mathbf{F}_i(t) \right| \leq C_H(\varepsilon_0)$$

for all $i = 1, \dots, N$ and all $t \geq t_0$, where

$$C_H(\varepsilon_0) = (N-1)^{\frac{1}{2}} A r_C + (N^2 - N)^{\frac{1}{2}} B \left(\varepsilon_0 + \frac{C_1}{K_v} \right) + N^{-\frac{1}{2}} C_1, \quad (55)$$

Viewing (54) as a linear non-homogeneous system, for given $i \in \{1, \dots, N\}$, we have

$$\begin{aligned} \mathbf{x}_i(t) &= \frac{e^{\lambda_1(t-t_0)}}{\lambda_2 - \lambda_1} [\lambda_2 \mathbf{x}_i(t_0) - \mathbf{w}_i(t_0)] + \frac{e^{\lambda_2(t-t_0)}}{\lambda_2 - \lambda_1} [-\lambda_1 \mathbf{x}_i(t_0) + \mathbf{w}_i(t_0)] \\ &+ \frac{1}{\lambda_2 - \lambda_1} \int_{t_0}^t [-e^{\lambda_1(t-\tau)} + e^{\lambda_2(t-\tau)}] M^{-1} \mathbf{H}_i(\tau) d\tau, \end{aligned} \quad (56)$$

$$\begin{aligned} \mathbf{w}_i(t) &= \frac{e^{\lambda_1(t-t_0)}}{\lambda_2 - \lambda_1} [\lambda_1 \lambda_2 \mathbf{x}_i(t_0) - \lambda_1 \mathbf{w}_i(t_0)] + \frac{e^{\lambda_2(t-t_0)}}{\lambda_2 - \lambda_1} [-\lambda_1 \lambda_2 \mathbf{x}_i(t_0) + \lambda_2 \mathbf{w}_i(t_0)] \\ &+ \frac{1}{\lambda_2 - \lambda_1} \int_0^t [-\lambda_1 e^{\lambda_1(t-\tau)} + \lambda_2 e^{\lambda_2(t-\tau)}] M^{-1} \mathbf{H}_i(\tau) d\tau, \end{aligned} \quad (57)$$

where

$$\lambda_{1,2} = \frac{-\tilde{K}_v \pm \sqrt{\tilde{K}_v^2 - 4\tilde{K}_p}}{2}. \quad (58)$$

Since the real parts of $\lambda_{1,2}$ are negative, first two terms in (56) and (57) vanish as $t \rightarrow \infty$, and therefore the asymptotic behavior of $\mathbf{x}_i(t)$ and $\mathbf{w}_i(t)$ is determined by the corresponding integral terms.

For $t \geq t_0$, for the integral term in (56), we have

$$\left| \frac{1}{\lambda_2 - \lambda_1} \int_{t_0}^t [-e^{\lambda_1(t-\tau)} + e^{\lambda_2(t-\tau)}] M^{-1} \mathbf{H}_i(\tau) d\tau \right| \leq \left| \frac{2(\lambda_1 + \lambda_2)}{(\lambda_2 - \lambda_1)\lambda_1\lambda_2} \right| M^{-1} C_H(\varepsilon_0),$$

and for the integral term in (57), we have

$$\left| \frac{1}{\lambda_2 - \lambda_1} \int_{t_0}^t [-\lambda_1 e^{\lambda_1(t-\tau)} + \lambda_2 e^{\lambda_2(t-\tau)}] M^{-1} \mathbf{H}_i(\tau) d\tau \right| \leq \frac{2}{|\lambda_2 - \lambda_1|} M^{-1} C_H(\varepsilon_0).$$

Then (i) and (ii) follow. \square

Remark 8. Let $\gamma = \frac{4\tilde{K}_p}{\tilde{K}_v^2}$. It follows from Theorem 3 that the coordinates of the i -th agent satisfy

$$|\mathbf{x}_i(t)| \leq \frac{2}{\tilde{K}_p \sqrt{|1 - \gamma|}} C_2 \nu, \quad |\mathbf{w}_i(t)| \leq \frac{2}{\tilde{K}_v \sqrt{|1 - \gamma|}} C_2 \nu, \quad (59)$$

for all $t \geq 0$, where $\nu > 1$ depends on $\mathbf{x}_i(0)$ and $\mathbf{w}_i(0)$ and does not depend on time. By tuning the parameters K_p and K_v , one might control the deviation of the agent's trajectory from that of the virtual leader. In particular, if $K_p \gg K_v$, so that $\gamma > 1$, the eigenvalues (58) become complex, so the dynamics of the agent will contain additional oscillations. At the same time, higher values of K_p will ensure a tighter bound on the agent's position. In turn, if

$K_p \ll K_v$, we get $\gamma < 1$ which makes the eigenvalues (58) real. Such a scenario will represent an “overdamped” system with fewer oscillations and shorter stabilization time. Notably, for γ being close to one, the bounds in (59) become small, and therefore it is possible to ensure a tight formation control of the group while using relatively small values of K_p and K_v . The case when γ is precisely one discussed in the theorem that follows.

For the case of repeated eigenvalue in (54), we can get a stronger result than that of the Theorem 3.

Theorem 4. *Let $(\mathbf{X}(t), \mathbf{W}(t))$ be a solution of (45). Suppose that Assumptions 1 and 2 hold, and that $\tilde{K}_v^2 - 4\tilde{K}_p = 0$. Then, for any $i = 1, \dots, N$,*

(i) *for any $\varepsilon_1 > 0$, there exists $t_1 = t_1(\mathbf{x}_i(0), \mathbf{w}_i(0), \varepsilon_1) \geq 0$ such that $|\mathbf{x}_i(t)| \leq \varepsilon_1 + \frac{4}{K_v} C_2$, for all $t \geq t_1$;*

(ii) *$|\mathbf{w}_i(t)| \rightarrow 0$, as $t \rightarrow \infty$.*

Proof. The proof is analogous to that of the Theorem 3. As before, consider the linear non-homogeneous system (54). When $\tilde{K}_v^2 - 4\tilde{K}_p = 0$, the corresponding linear homogeneous system has a single repeated eigenvalue $\lambda = -\frac{\tilde{K}_v}{2}$.

Fix $\varepsilon_0 > 0$. For given $i \in \{1, \dots, N\}$, we have

$$\begin{aligned} \mathbf{x}_i(t) &= e^{\lambda(t-t_0)} [(-\lambda(t-t_0) + 1) \mathbf{x}_i(t_0) + (t-t_0) \mathbf{w}_i(t_0)] + \\ &+ \int_{t_0}^t e^{\lambda(t-\tau)} (t-\tau) M^{-1} \mathbf{H}_i(\tau) d\tau, \end{aligned} \quad (60)$$

$$\begin{aligned} \mathbf{w}_i(t) &= e^{\lambda(t-t_0)} [-\lambda^2(t-t_0) \mathbf{x}_i(t_0) + (\lambda(t-t_0) + 1) \mathbf{w}_i(t_0)] + \\ &+ \int_{t_0}^t e^{\lambda(t-\tau)} [\lambda(t-\tau) + 1] M^{-1} \mathbf{H}_i(\tau) d\tau, \end{aligned} \quad (61)$$

where $t_0 = t_0(\mathbf{W}(0), \varepsilon_0) \geq 0$ is such that $|\mathbf{H}_i(t)| \leq C_H(\varepsilon_0)$, for all $i = 1, \dots, N$ and all $t \geq t_0$, with $C_H(\varepsilon_0)$ is as defined by (55).

Since $\lambda < 0$, the first terms in (60) and (61) vanish as $t \rightarrow \infty$, and therefore the asymptotic behavior of $\mathbf{x}_i(t)$ and $\mathbf{w}_i(t)$ is determined by the corresponding integral terms.

For $t \geq t_0$, for the integral term in (56), we have

$$\left| \int_{t_0}^t e^{\lambda(t-\tau)} (t-\tau) M^{-1} \mathbf{H}_i(\tau) d\tau \right| \leq \left[e^{\lambda(t-t_0)} \left(\frac{1}{\lambda} (t-t_0) - \frac{1}{\lambda^2} \right) + \frac{1}{\lambda^2} \right] M^{-1} C_H(\varepsilon_0)$$

and for the integral term in (57), we have

$$\left| \int_{t_0}^t e^{\lambda(t-\tau)} [\lambda(t-\tau) + 1] M^{-1} \mathbf{H}_i(\tau) d\tau \right| \leq e^{\lambda(t-t_0)} (t-t_0) M^{-1} C_H(\varepsilon_0).$$

Then (i) and (ii) follow. □

The results of the above theorems are summarized in the following Corollary.

Corollary 1. *Suppose Assumptions 1 and 2 hold. Then, the group of agents exhibits approximate proper flocking. If, in addition, $\tilde{K}_v^2 - 4\tilde{K}_p = 0$, the flocking is exact.*

Remark 9. Suppose one wants to incorporate stochastic effects into the agent interactions by adding a random force \mathbf{f}_i^R , $i = 1, \dots, N$, to (1). If $\mathbf{f}_i^R(t)$, $t \geq 0$, viewed as a realization of some stochastic process, is always C^1 and bounded, then Theorems 3 and 4 will still hold. This could be easily seen from the fact that \mathbf{f}^L was merely required to be bounded (in addition to our initial assumptions of being C^1) in the proofs of either of the above theorems. Thus, if another bounded term \mathbf{f}_i^R is added to the right-hand side of (1), Theorem 3 will still guarantee that the solutions are (almost surely) bounded. Similarly, for the case of repeated eigenvalue, the system will still (almost surely) exhibit proper flocking due to Theorem 4.

Remark 10. Let $\eta > 0$. It follows from Theorem 3 that, for $\tilde{K}_v^2 - 4\tilde{K}_p^2 \neq 0$, there exists a set

$$\mathcal{B} = \left\{ (\mathbf{X}, \mathbf{W}) \in \mathbb{R}^{2nd} : |\mathbf{x}_i| \leq \frac{2(1+\eta)\tilde{K}_v}{\tilde{K}_p \sqrt{|\tilde{K}_v^2 - 4\tilde{K}_p^2|}} C_2, \quad |\mathbf{w}_i| \leq \frac{2(1+\eta)}{\sqrt{|\tilde{K}_v^2 - 4\tilde{K}_p^2|}} C_2, \quad 1 \leq i \leq N \right\},$$

such that, for any bounded set $\mathcal{B}_0 \subseteq \mathbb{R}^{2nd}$, an orbit starting in \mathcal{B}_0 enters \mathcal{B} after some time $t_1 = t_1(\mathcal{B}_0)$. In other words, \mathcal{B} is a global absorbing set for (13). Since \mathcal{B} is bounded, (13) possesses a global (compact) attractor (see, e.g., [48]). Similarly, for $\tilde{K}_v^2 - 4\tilde{K}_p^2 = 0$, Theorem 4 guarantees the existence of a global bounded absorbing set

$$\mathcal{B} = \left\{ (\mathbf{X}, \mathbf{W}) \in \mathbb{R}^{2nd} : |\mathbf{x}_i| \leq \frac{4(1+\eta)}{\tilde{K}_v} C_2, \quad |\mathbf{w}_i| \leq \eta, \quad i = 1, \dots, N \right\}.$$

Thus (13) possesses a global attractor for any configuration of the control parameters \tilde{K}_p and \tilde{K}_v .

5.2 Exact flocking

Suppose that $\tilde{K}_v^2 - 4\tilde{K}_p \neq 0$. To show that the system exhibits exact flocking in this case, introduce a new coordinate system centered at the center of mass of the group $(\bar{\mathbf{x}}, \bar{\mathbf{w}}) = \left(\sum_{i=1}^N \bar{\mathbf{x}}_i, \sum_{i=1}^N \bar{\mathbf{w}}_i \right)$ by defining

$$\hat{\mathbf{x}}_i = \mathbf{x}_i - \bar{\mathbf{x}}, \quad \hat{\mathbf{w}}_i = \mathbf{w}_i - \bar{\mathbf{w}}, \quad i = 1, \dots, N,$$

and $\hat{\mathbf{X}} = (\hat{\mathbf{x}}_1, \dots, \hat{\mathbf{x}}_N)$, $\hat{\mathbf{W}} = (\hat{\mathbf{w}}_1, \dots, \hat{\mathbf{w}}_N)$. As before, we have $\hat{\mathbf{x}}_i - \hat{\mathbf{x}}_j = \mathbf{x}_i - \mathbf{x}_j$ and $\hat{\mathbf{w}}_i - \hat{\mathbf{w}}_j = \mathbf{w}_i - \mathbf{w}_j$, for all $i, j = 1, \dots, N$. Then, the dynamics of the center of mass is given by

$$\begin{aligned} \dot{\hat{\mathbf{x}}} &= \bar{\mathbf{w}}, \\ M\dot{\bar{\mathbf{w}}} &= \frac{1}{N} \sum_{i=1}^N \mathbf{u}^P(\bar{\mathbf{x}} + \hat{\mathbf{x}}_i) + \frac{1}{N} \sum_{i=1}^N \mathbf{u}^V(\bar{\mathbf{w}} + \hat{\mathbf{w}}_i) - M\mathbf{f}^L \end{aligned} \tag{62}$$

and the dynamics of the agents relative to the center of mass is given by

$$\begin{aligned}\dot{\hat{\mathbf{x}}}_i &= \hat{\mathbf{w}}_i, \\ M\dot{\hat{\mathbf{w}}}_i &= \mathbf{f}_i^C + \mathbf{f}_i^D + \mathbf{u}^P(\bar{\mathbf{x}} + \hat{\mathbf{x}}_i) + \mathbf{u}^V(\bar{\mathbf{w}} + \hat{\mathbf{w}}_i) - \frac{1}{N} \sum_{j=1}^N \mathbf{u}^P(\bar{\mathbf{x}} + \hat{\mathbf{x}}_j) - \frac{1}{N} \sum_{j=1}^N \mathbf{u}^V(\bar{\mathbf{w}} + \hat{\mathbf{w}}_j),\end{aligned}\tag{63}$$

$i = 1, \dots, N$.

We now make the assumption that the activation threshold r_0 of the position alignment self-propulsion force is sufficiently large.

Assumption 3.

$$r_0 > \frac{2\tilde{K}_v}{\tilde{K}_p \sqrt{|\tilde{K}_v^2 - 4\tilde{K}_p|}} C_2.$$

The above assumption along with Theorem 3 (i) imply that there exists t_1 such that

$$|\mathbf{x}_i(t)| \leq r_0, \quad i = 1, \dots, N,\tag{64}$$

for all $t \geq t_1$, and therefore the position alignment self-propulsion force vanishes for $t \geq t_1$. Suppose that t_1 is the smallest time such that (64) holds for all $t \geq t_1$. In this case, we would refer to t_1 as the *spatial stabilization time*.

Let $D\delta\mathbf{u}^V(\mathbf{y})$ denote the Jacobian of $\delta\mathbf{u}^V$ at $\mathbf{y} \in \mathbb{R}^d$. We now impose an additional assumption on the non-linear term of the velocity alignment self-propulsion force.

Assumption 4. *There exists $C_{\delta V}$, such that $|D\delta\mathbf{u}^V(\mathbf{y})| \leq C_{\delta V}$, for all $\mathbf{y} \in \mathbb{R}^d$.*

Note that, whenever Assumptions 1 and 2 hold, velocities of the agents are bounded, so $\delta\mathbf{u}^V$ take values from a compact subset of \mathbb{R}^d . Then $|D\delta\mathbf{u}^V(\mathbf{w}_i(t))|$ will be bounded, for all $i = 1, \dots, N$, and all $t \geq 0$, provided \mathbf{u}^V is C^1 .

First, consider the dynamics of the agents relative to the center of mass. For $t \geq t_1$, the second equation in (63) becomes

$$M\dot{\hat{\mathbf{w}}}_i = \mathbf{f}_i^C + \mathbf{f}_i^D - K_v \hat{\mathbf{w}}_i + \delta\mathbf{u}^V(\bar{\mathbf{w}} + \hat{\mathbf{w}}_i) - \frac{1}{N} \sum_{j=1}^N \delta\mathbf{u}^V(\bar{\mathbf{w}} + \hat{\mathbf{w}}_j), \quad i = 1, \dots, N.$$

Using a first-order Taylor expansion of $\delta\mathbf{u}^V$ at $\bar{\mathbf{w}}$, we get

$$M\dot{\hat{\mathbf{w}}}_i = \mathbf{f}_i^C + \mathbf{f}_i^D - K_v \hat{\mathbf{w}}_i + D\delta\mathbf{u}^V(\boldsymbol{\zeta}_i) \hat{\mathbf{w}}_i - \frac{1}{N} \sum_{j=1}^N D\delta\mathbf{u}^V(\boldsymbol{\zeta}_j) \hat{\mathbf{w}}_j, \quad i = 1, \dots, N,$$

for all $t \geq t_1$, where $\boldsymbol{\zeta}_i \in \mathbb{R}^d$, $i = 1, \dots, N$, belongs to the line segment connecting $\bar{\mathbf{w}}$ and $\hat{\mathbf{w}}_i$. Then, for $t \geq t_1$, (63) could be written as

$$\begin{aligned}\dot{\hat{\mathbf{X}}} &= \hat{\mathbf{W}}, \\ M\dot{\hat{\mathbf{W}}} &= -\nabla_{\hat{\mathbf{X}}} U(\hat{\mathbf{X}}) - L(\hat{\mathbf{X}}) \hat{\mathbf{W}} - K_v \hat{\mathbf{W}} + \Delta(t) \hat{\mathbf{W}}\end{aligned}\tag{65}$$

where $\Delta(t)$ is a block matrix with $N \times N$ blocks of size $d \times d$ with (i, j) -th block given by

$$[\Delta(t)]_{i,j} = \begin{cases} (1 - \frac{1}{N})D\delta\mathbf{u}^V(\boldsymbol{\zeta}_i(t)), & \text{if } i = j, \\ \frac{1}{N}D\delta\mathbf{u}^V(\boldsymbol{\zeta}_j(t)), & \text{otherwise.} \end{cases}$$

Note that Assumption 4 implies that

$$|\Delta(t)| \leq C_3,$$

for all $t \geq t_1$, where

$$C_3 = [2(N-1)]^{\frac{1}{2}} C_{\delta V}.$$

As before, for the reduced system

$$\begin{aligned} \dot{\hat{\mathbf{X}}} &= \hat{\mathbf{W}}, \\ M\dot{\hat{\mathbf{W}}} &= -\nabla_{\hat{\mathbf{X}}}U(\hat{\mathbf{X}}) - L(\hat{\mathbf{X}})\hat{\mathbf{W}} - K_v\hat{\mathbf{W}}, \end{aligned} \tag{66}$$

we can show that the velocities decay exponentially.

Lemma 5. *Let $(\hat{\mathbf{X}}(t), \hat{\mathbf{W}}(t))$ be a solution of the reduced system (66). Then*

$$|\hat{\mathbf{W}}(t)| \leq |\hat{\mathbf{W}}(t_1)|e^{-\frac{K_v}{M}(t-t_1)},$$

for all $t \geq t_1$.

Proof. The proof is identical to that of the Lemma 3 if one replaces (48) with

$$E_r(\hat{\mathbf{X}}, \hat{\mathbf{W}}) = \frac{1}{2}M|\hat{\mathbf{W}}|^2 + U(\hat{\mathbf{X}}).$$

□

We can now prove another key result of this section.

Theorem 5. *Let $(\hat{\mathbf{X}}(t), \hat{\mathbf{W}}(t))$ be a solution of (65). Suppose Assumption 4 hold. Then, for all $i = 1, \dots, N$,*

$$(i) \quad |\hat{\mathbf{x}}_i(t) - \hat{\mathbf{x}}_i(t_1)| \leq |\hat{\mathbf{W}}(t_1)| \left[\frac{M}{2\hat{K}} \left(1 - e^{-\frac{2\hat{K}}{M}(t-t_1)} \right) \right]^{\frac{1}{2}};$$

$$(ii) \quad |\hat{\mathbf{w}}_i(t)| \leq |\hat{\mathbf{W}}(t_1)|e^{-\frac{\hat{K}}{M}(t-t_1)};$$

for all $t \geq t_1$, where

$$\hat{K} = K_v - C_3.$$

Proof. Let $\hat{\Psi}(t, s)$, $t \geq s \geq 0$ be the transition matrix of the linear system (66). By the variation of constants formula, the solution of (65) is given by

$$(\hat{\mathbf{X}}(t), \hat{\mathbf{W}}(t)) = \hat{\Psi}(t, t_1)(\hat{\mathbf{X}}(t_1), \hat{\mathbf{W}}(t_1)) + \int_{t_1}^t \hat{\Psi}(t, \tau)(\mathbf{0}, M^{-1}\Delta(\tau)\hat{\mathbf{W}}(\tau))d\tau.$$

As before, let $\hat{\Psi}_{\mathbf{W}}(t, s)$ be the last Nd rows of the matrix $\hat{\Psi}(t, s)$. Using Lemma 5, we get

$$\begin{aligned} |\hat{\mathbf{W}}(t)| &\leq |\hat{\Psi}_{\mathbf{W}}(t, t_1)(\hat{\mathbf{X}}(t_1), \hat{\mathbf{W}}(t_1))| + \left| \int_{t_1}^t \hat{\Psi}_{\mathbf{W}}(t, \tau)(\mathbf{0}, M^{-1}\Delta(\tau)\hat{\mathbf{W}}(\tau))d\tau \right| \\ &\leq |\hat{\mathbf{W}}(t_1)|e^{-\frac{K_v}{M}(t-t_1)} + \int_{t_1}^t M^{-1}C_3|\hat{\mathbf{W}}(\tau)|e^{-\frac{K_v}{M}(t-t_1)}d\tau. \end{aligned} \quad (67)$$

Let $\Lambda(t) = |\hat{\mathbf{W}}(t)|e^{\frac{K_v}{M}t}$. Then (67) could be written as

$$\Lambda(t) \leq \Lambda(t_1) + \int_{t_1}^t M^{-1}C_3\Lambda(\tau)d\tau.$$

By Grönwall's inequality, we get

$$\Lambda(t) \leq \Lambda(t_1) \exp \left(\int_{t_1}^t M^{-1}C_3d\tau \right).$$

Thus

$$|\hat{\mathbf{W}}(t)| \leq |\hat{\mathbf{W}}(t_1)| \exp \left(-\frac{1}{M} (K_v - C_3) (t - t_1) \right),$$

and (ii) follows.

Now, using Jensen's inequality, for any $i = 1, \dots, N$, we get

$$\begin{aligned} |\hat{\mathbf{x}}_i(t) - \hat{\mathbf{x}}_i(t_1)|^2 &= \sum_{m=1}^d \left| \hat{\mathbf{x}}_i^{(m)}(t) - \hat{\mathbf{x}}_i^{(m)}(t_1) \right|^2 \\ &= \sum_{m=1}^d \left| \int_{t_1}^t \hat{\mathbf{w}}_i^{(m)}(\tau)d\tau \right|^2 \\ &\leq \int_{t_1}^t |\hat{\mathbf{w}}_i(\tau)|^2 d\tau \\ &\leq |\hat{\mathbf{W}}(t_1)|^2 \int_{t_1}^t e^{-\frac{2\hat{K}}{M}(\tau-t_1)}d\tau \\ &\leq |\hat{\mathbf{W}}(t_1)|^2 \frac{M}{2\hat{K}} \left(1 - e^{-\frac{2\hat{K}}{M}(t-t_1)} \right), \end{aligned} \quad (68)$$

and (i) follows. □

Corollary 2. *Suppose Assumptions 1-4 hold and that $\hat{K} > 0$. Then*

- (i) after the spatial stabilization time, the agents' positions will not change by more than $|\hat{\mathbf{W}}(t_1)| \left(\frac{M}{\hat{K}}\right)^{\frac{1}{2}}$;
- (ii) $|\mathbf{w}_i(t) - \bar{\mathbf{w}}(t)| \rightarrow 0$ as $t \rightarrow \infty$, for all $i = 1, \dots, N$, and the group exhibits exact flocking;

Proof. Since $\hat{K} > 0$, (i) follows from Theorem 5 (i), and (ii) follows from Theorem 5 (ii) and Theorem 3 (i). \square

Remark 11. The rate of convergence to the velocity consensus as well as spatial stability of the group depend on \hat{K} , which, in turn, depends on the tunable parameters K_v and $C_{\delta V}$. Informally speaking, the former represents the magnitude of the linear component of the velocity alignment self-propulsion force, and the latter represents the magnitude of its non-linear part. The stronger the linear component of the force, the faster the group will converge to a velocity consensus and the more rigid spatial configuration it will maintain.

5.3 Dynamics of the center of mass

Now, consider the dynamics of the center of mass. For $t \geq t_1$, (62) could be written as

$$\begin{aligned} \dot{\bar{\mathbf{x}}} &= \bar{\mathbf{w}}, \\ M\dot{\bar{\mathbf{w}}} &= -K_v \bar{\mathbf{w}} + \frac{1}{N} \sum_{i=1}^N \delta \mathbf{u}^V(\bar{\mathbf{w}} + \hat{\mathbf{w}}_i) - M\mathbf{f}^L \end{aligned} \quad (69)$$

We show that the deviation of the velocity of the center of mass from that of the virtual leader stays bounded after the spatial stabilization time.

Theorem 6. Let $(\bar{\mathbf{x}}(t), \bar{\mathbf{w}}(t))$ be a solution of (69). Suppose Assumption 4 hold. Then, for any $\varepsilon_2 > 0$, there exists $t_2 = t_2(\bar{\mathbf{w}}(t_1), \varepsilon_2)$ such that

$$|\bar{\mathbf{w}}(t)| \leq \varepsilon_2 + \frac{2C_4}{K_v}, \quad (70)$$

for all $t \geq t_2$, where

$$C_4 = N^{\frac{1}{2}} C_{\delta V} + M C_l$$

Proof. Note that (69) is decoupled, so in order to obtain (70) it suffices to consider the second equation in (69) only. As before, a solution $\bar{\mathbf{w}}_r(t)$ of the linear reduced system

$$M\dot{\bar{\mathbf{w}}}_r = -K_v \bar{\mathbf{w}}_r \quad (71)$$

will satisfy

$$|\bar{\mathbf{w}}_r(t)| \leq |\bar{\mathbf{w}}_r(t_1)| e^{-\frac{K_v}{M}(t-t_1)},$$

for all $t \geq t_1$. Let $\Psi_{\bar{\mathbf{w}}}(t, s)$, $t \geq s \geq 0$ be the transition matrix of (71). Then, by the variation of constants formula, we get

$$\begin{aligned} |\bar{\mathbf{w}}(t)| &= \left| \Psi_{\bar{\mathbf{w}}}(t, t_1) \bar{\mathbf{w}}(t_1) + \int_{t_1}^t \Psi_{\bar{\mathbf{w}}}(t, \tau) \left(\frac{1}{NM} \sum_{i=1}^N \delta \mathbf{u}^V(\bar{\mathbf{w}} + \hat{\mathbf{w}}_i) - \mathbf{f}^L(\tau) \right) d\tau \right| \\ &\leq |\bar{\mathbf{w}}_r(t_1)| e^{-\frac{K_v}{M}(t-t_1)} + \frac{1}{M} \int_{t_1}^t \left| \frac{1}{N} \sum_{i=1}^N \delta \mathbf{u}^V(\bar{\mathbf{w}} + \hat{\mathbf{w}}_i) - M \mathbf{f}^L(\tau) \right| e^{-\frac{K_v}{M}(t-\tau)} d\tau \\ &\leq \left(|\bar{\mathbf{w}}_r(t_1)| - \frac{C_4}{K_v} \right) e^{-\frac{K_v}{M}(t-t_1)} + \frac{C_4}{K_v}. \end{aligned}$$

Since $K_v > 0$, the result follows. \square

Remark 12. For the case $\tilde{K}_v^2 - 4\tilde{K}_p \neq 0$, for large times, Corollary 2 together with Theorem 6 can potentially provide a tighter bound on $|\mathbf{w}_i(t)|$, $i = 1, \dots, N$, than the one suggested in Theorem 3 (ii). However, which bound is tighter would depend on the relation between the tunable parameters K_p, K_v, C_p, C_l , and $C_{\delta V}$.

6 Computational examples

In this section, we first present results of numerical simulations demonstrating that the system exhibits flocking dynamics in both dissipative and non-dissipative cases. We discuss various qualitatively distinct regimes of motion that could be achieved using different combinations of the control parameters. Finally, we provide some numerical illustrations of wobblers, the non-equilibrium solutions that can be a part of the attractor in the non-strictly dissipative case.

Non-dimensional units. For numerical simulations, it would be convenient to introduce non-dimensional units allowing to work with numerical values of order of unity and obtain some characteristic quantities defining different regimes of motion. Let

$$m' = \frac{[m]}{M}, \quad r' = \frac{[r]}{r_C}, \quad v' = \frac{[v]}{v_{char}}, \quad t' = \frac{[t]}{r_C/v_{char}},$$

where v_{char} is the characteristic speed of the virtual leader (and thus the characteristic speed of all the agents in the group, assuming that the agents are following the leader's trajectory). Plugging the above into (1), we get

$$\begin{aligned} \dot{\mathbf{q}}'_i &= \mathbf{v}'_i, \\ \dot{\mathbf{v}}'_i &= A' \sum_{i \neq j} w_C(r_C |\mathbf{q}'_{ij}|) \mathbf{q}'_{ij} - B' \sum_{i \neq j} w_D(r_D |\mathbf{q}'_{ij}|) \mathbf{v}'_{ij} \\ &\quad - \alpha' k(r_C |\mathbf{q}'_{il}|) \frac{\mathbf{q}'_{il}}{|\mathbf{q}'_{il}|} - \beta' p(v_{char} |\mathbf{v}'_{il}|) \frac{\mathbf{v}'_{il}}{|\mathbf{v}'_{il}|}, \end{aligned} \quad i = 1, \dots, N,$$

where $\mathbf{q}'_i = r_C^{-1} \mathbf{q}_i$, $\mathbf{v}'_i = v_{char}^{-1} \mathbf{v}_i$, for $i = 1, \dots, N + 1$. The dimensionless parameters

$$A' = \frac{r_C^2}{M v_{char}^2} A, \quad B' = \frac{r_C}{M v_{char}} B, \quad \alpha' = \frac{r_C^2}{M v_{char}^2} \alpha, \quad \beta' = \frac{r_C}{M v_{char}} \beta \quad (72)$$

represent relative contributions of the corresponding forces to the dynamics of an agent, the parameters

$$r'_D = \frac{r_D}{r_C}, \quad r'_0 = \frac{r_0}{r_C}$$

represent the cut-off distance of the ambient dissipative force and the activation threshold of the self-propulsion position alignment force, respectively, measured in terms of the cut-off distance of the ambient conservative force, and the parameter

$$v'_0 = \frac{v_0}{v_{char}}$$

represents the activation threshold of the self-propulsion velocity alignment force measured in terms of the characteristic speed of the virtual leader.

Working with the non-dimensional units introduced above, we set $A' = 10$ and $r'_D = 5$. The remaining dimensionless parameters B' , α' , r'_0 , β' , and v'_0 are assumed to be free and are varied to obtain different regimes of motions. We use velocity-Verlet [?] integration scheme implemented in a custom simulator setting the time step to $\Delta t = 10^{-2}$ and running each simulation for $n = 10^5$ steps which were determined to be sufficient for the system to stabilize under considered scenarios.

Regimes of motion. We consider 9 different regimes of motion, listed in Table 1, that are defined by various combinations of free parameters.

Regime	Parameters					ρ	v_b
	B'	α'	r'_0	β'	v'_0		
(1) typical	1	1	4.64	1	0.5	0.25	1
(2) no velocity alignment	1	1	4.64	0	0	0.25	1
(3) tight velocity alignment	1	1	4.64	1	0	0.25	1
(4) no position alignment	1	0	4.64	1	0	0.25	1
(5) low density	10	1	7.93	1	0.5	0.1	1
(6) optimal density	10	1	3.23	1	0.5	0.74	1
(7) high density	10	1	2.32	1	0.5	2	1
(8) low speed	0.2	1	4.64	0.2	0.5	0.25	0.2
(9) high speed	5	1	4.64	5	0.5	0.25	2

Table 1: Regimes of motion and corresponding values of the free parameters for a group of $N = 100$ agents in a 3-dimensional space with $A/B = 10$.

The quantities

$$\rho = \frac{N V_d(0.5)}{V_d(r'_0)}, \quad v_b = \frac{v_0}{r_C},$$

where $V_d(r)$ is the volume of a d -dimensional ball of radius $r > 0$, are derived from the free parameters and could be used to characterize qualitatively different regimes of motion. The position alignment self-propulsion force, pushing agents towards the position of the virtual leader whenever they are farther than r'_0 from it, would make the group tend to stay within the ball $B(\mathbf{q}'_l(t'), r'_0)$. Therefore, assuming that the quantity ρ could be thought of as a “density” of the group, with higher values characterizing a “tighter packing” resulting in a significant presence of both ambient and self-propulsion conservative forces, and lower values characterizing a “looser packing” with a weaker influence of ambient forces. In turn, the quantity v_b represents the characteristic speeds of the virtual leader measured in body length per second (blps) [41]. It could be seen from (72) that $A'/B' = v_b^{-1}A/B$, where A/B is a fixed quantity since it only depends on the material of the elastic bumpers and the properties of the liquid the group is submerged into. Thus, by varying the ratio A'/B' , one can implement scenarios with different characteristic speed of the virtual leader. In our simulations, we put $A/B = 10$.

Regime (1) is characterized by the presence of both the position alignment force and the velocity alignment force as well as by moderate density of the agents, and is assumed to be typical. Also, in this regime, velocity alignment is not “tight” by which we mean that the corresponding force is activated only when an agent’s velocity deviation from that of the virtual is sufficiently large. In regimes (2)-(4), we disable either of the position and the velocity alignment forces as well as “tighten” the velocity alignment. In regimes (5)-(7), we vary the density of the group keeping the rest of the parameters fixed. Note that we refer to the density $\rho = 0.74$ as the optimal one since it is approximately equal to the maximum density for the packing of a collection of identical balls in \mathbb{R}^3 [13]. Thus, for any $\rho < 0.74$, it is guaranteed that the ambient conservative is non-zero for at least one pair of agents. Finally, in regimes (8)-(9), we vary characteristic speed of the group.

We put $k(s) = p(s) = s$ in (6), so that the position and the velocity alignment self-propulsion forces become linear, but only on their support. Although the above results in g and h failing to be C^1 , we assume that $k(s) = p(s) = s$ are approximations of a C^1 function that is equal to the identity function everywhere except for an interval containing the origin, which is negligibly small for numerical simulations.

Flocking. As before, we distinguish two possible scenarios: dissipative and non-dissipative. To simulate the dissipative scenario, we let the virtual leader move along a straight line with the constant speed v_{char} . For the non-dissipative scenario, the leader moves along a circle of radius $10r'_0$ with the constant speed v_{char} . The simulations are performed for $d = 3$ and $N = 100$ with the initial positions of the agents being randomly sampled from the uniform distribution on $B(\mathbf{q}'_l(0), r'_{init})$, and the initial velocities being randomly sampled from the d -variate truncated normal distribution with mean $\mathbf{v}'_l(0)$, covariance matrix I_d supported on the ball $B(\mathbf{v}'_l(0), 1)$. Here, we set $r'_{init} = 10$, which results in the initial spatial configuration of the group to have density $\rho = 0.025$.

In the process of simulations we measure the following quantities:

$$\bar{q}_{dev}(t') = \frac{1}{N} \sum_{i=1}^N |\mathbf{q}'_i(t') - \mathbf{q}'_l(t')|,$$

$$\bar{v}_{dev}(t') = \frac{1}{N} \sum_{i=1}^N |\mathbf{v}'_i(t') - \mathbf{v}'_l(t')|,$$

and

$$\begin{aligned} \bar{U}(t') &= \frac{1}{N} \sum_{i=1}^N \int_0^{t'} |\mathbf{u}'_i(\tau)| d\tau \\ &= \frac{1}{N} \sum_{i=1}^N \int_0^{t'} \left| \alpha' k(r_C |\mathbf{q}_{il}(\tau)|) \frac{\mathbf{q}'_{il}(\tau)}{|\mathbf{q}'_{il}(\tau)|} + \beta' p(v_{char} |\mathbf{v}'_{il}(\tau)|) \frac{\mathbf{v}'_{il}(\tau)}{|\mathbf{v}'_{il}(\tau)|} \right| d\tau. \end{aligned}$$

Here, $\bar{q}_{dev}(t')$ and $\bar{v}_{dev}(t')$ represent the average deviation of an agent's position and velocity, respectively, from the ones of the virtual leader at time $t' \geq 0$. Assuming that an agent is set in motion by a propeller powered by a DC motor connected to a battery, $\bar{U}(t')$ would represent the total battery drain (see Appendix B for details) at time $t' \geq 0$ averaged over all agents in the group. The results of simulations for the dissipative and the non-dissipative scenarios are shown in Figures 1 and 2, respectively.

It could be seen from the figures that in all of the regimes the relative positions of the agents stay bounded. In the dissipative scenario, a complete asymptotic velocity agreement is achieved in all of the regimes implying that the system exhibits proper asymptotic flocking. The same is true for the non-dissipative scenario in regimes (3) and (4). In all other regimes under the non-dissipative scenario, merely bounded velocity disagreement is achieved making the proper asymptotic flock only approximate. Thus, we conclude that applying "tight" velocity alignment is essential and its presence guarantees that the system will converge to a proper asymptotic flocking in any of the considered scenarios.

Notably, the absence of position alignment force is associated with a faster convergence to velocity agreement provided with a "tight" velocity control being applied (see regimes (3) and (4)). Yet, at the same time, spatial deviation of the group might be unacceptable for practical applications and therefore a balanced combination of the two alignment forces should be used, e.g., as in regime (1). From the point of view of the battery drain, regimes where the position alignment force is absent, are more preferable. A more detailed discussion of this aspect is presented in the next section.

Regimes with high values of the group density ρ tend to exhibit faster convergence to a velocity agreement yet are characterized by a more volatile spatial configuration. The former is the result of a stronger damping effect of the ambient dissipative force, whereas the latter is the outcome of an intense counteraction between the ambient conservative force and the position alignment self-propulsion force. In turn, higher values of v_b lead to higher volatility in both positions and velocities.

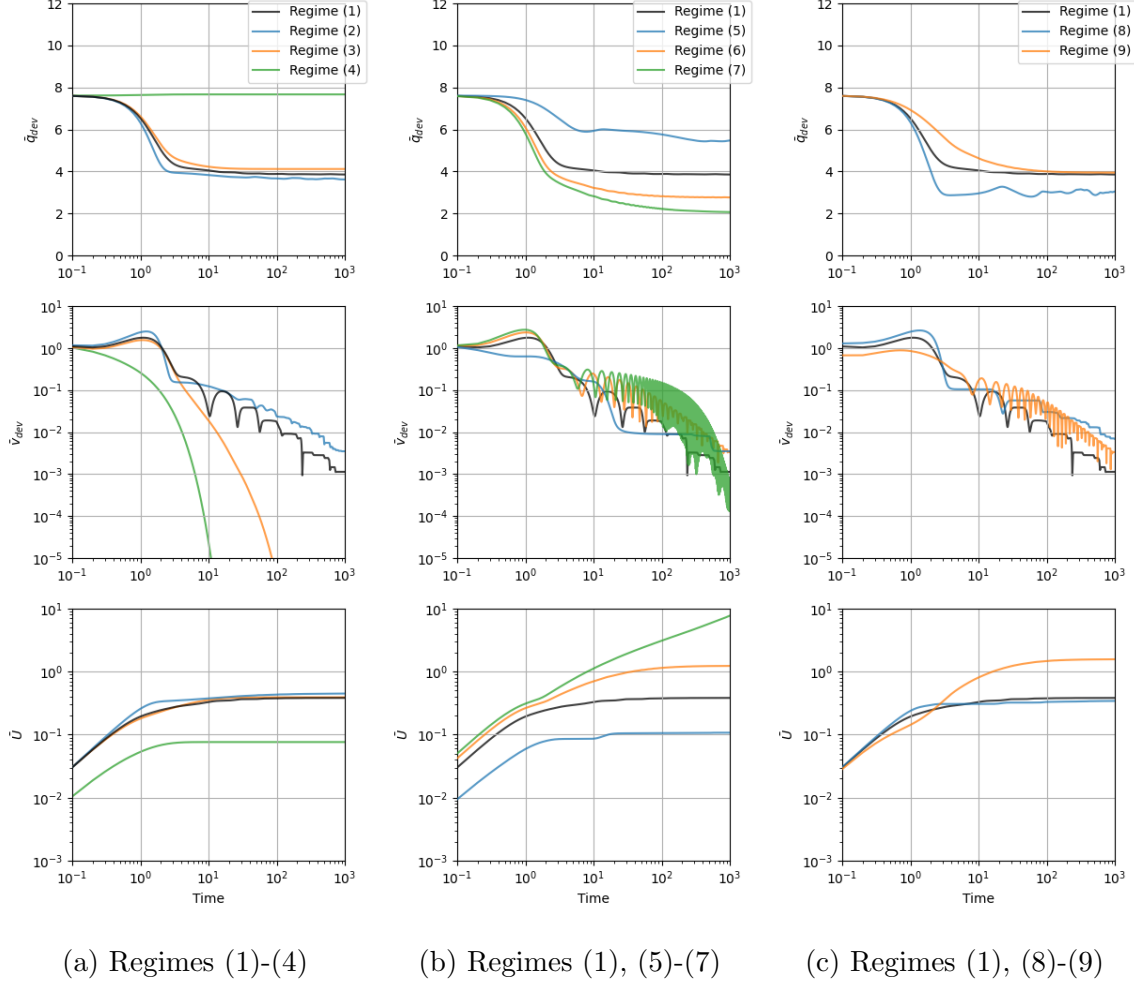


Figure 1: Measurements of $\bar{q}_{dev}(t')$, $\bar{v}_{dev}(t')$ and $\bar{U}(t')$ for the dissipative scenario for a group of $N = 100$ agents. The colored lines represent corresponding measurements for different regimes of motion.

Wobblers. To illustrate the results obtained in Section 5, we perform simulations of the dissipative scenario for a group of $N = 3$ agents moving in regimes (1) and (3) with r'_0 set to zero. Figure 3 shows the evolution of the differences of agents' positions as well as the agents' velocities. Whereas in both cases the spatial formation of the group converges to a static configuration, the asymptotic behavior of agents' velocities is qualitatively different in the two regimes. In regime (1), $v_0 = 0.5$ so that the explicit periodic solution given by (44) is observed in the velocity plot of Figure 3 (a). In turn, regime (3) has $v_0 = 0$ implying that the system converges to an equilibrium solution (see Theorem 1), which could be observed in Figure 3 (b).

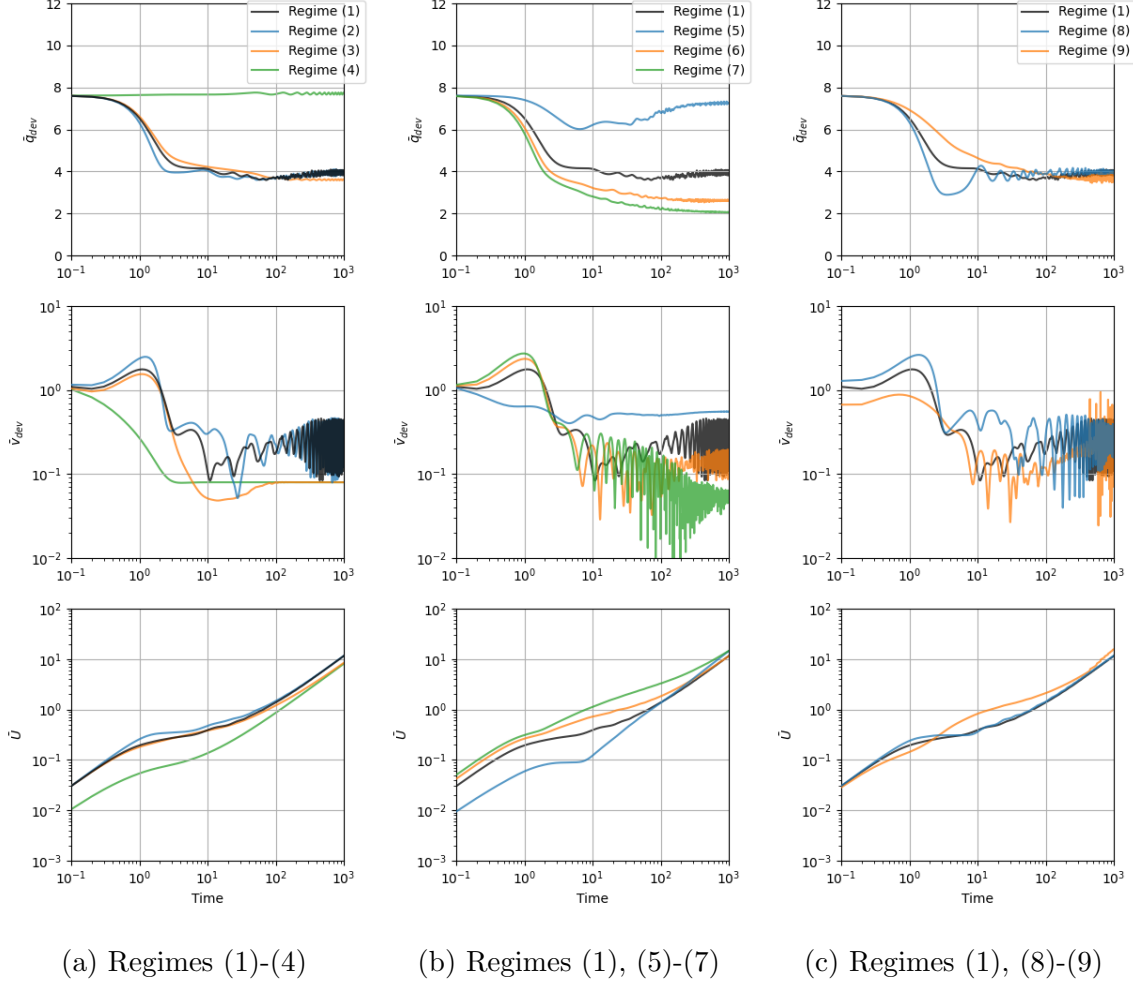


Figure 2: Measurements of $\bar{q}_{dev}(t')$, $\bar{v}_{dev}(t')$ and $\bar{U}(t')$ for the non-dissipative scenario for a group of $N = 100$ agents. The colored lines represent corresponding measurements for different regimes of motion.

7 Energy-efficient configurations of the self-propulsion forces

The purpose of this section is to investigate how adjusting the control parameters of self-propulsion forces affects the energy efficiency of the agents' movement. Using the parameters configuration that allows the group to follow a specified target trajectory with minimum energy consumption will result in a slower battery drain and will maximize the autonomous operational time of the group. Thus, identifying such parameter configuration is an important problem.

Working with the non-dimensional units introduced in the previous section, let $\Gamma = \{(\mathbf{q}'_i(t'), \mathbf{v}'_i(t')), 0 \leq t' \leq T'\}$ be a target trajectory that the group needs to follow in order

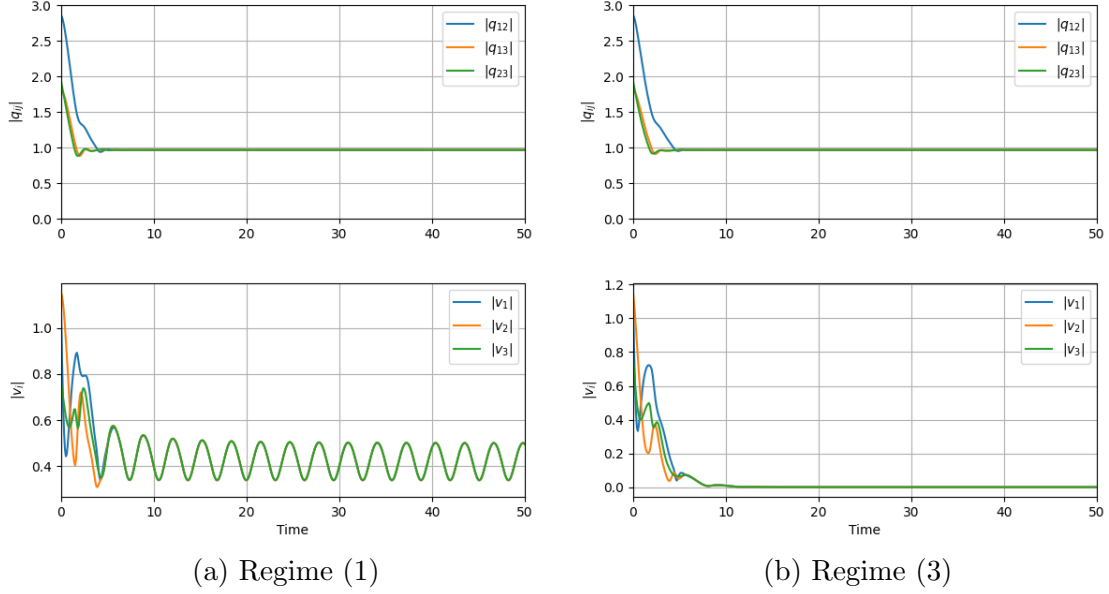


Figure 3: Differences of agents' positions and agents' velocities for a group of $N = 3$ agents moving in regimes (1) and (3) with $r_0 = 0$. The colored lines represent corresponding measurements for different agents.

to accomplish a certain task, where $T' > 0$ is the terminal time of the task. Let $\boldsymbol{\theta} = (\alpha', r'_0, \beta', v'_0) \in \Theta$ denote the vector of the control parameters of the self-propulsion forces, where $\Theta \subseteq \mathbb{R}^4$ is the set of feasible values, and let $(\mathbf{q}'_i(t'; \boldsymbol{\theta}), \mathbf{v}'_i(t'; \boldsymbol{\theta})), 0 \leq t \leq T$, be the solution of (6) subject to some initial conditions $(\mathbf{Q}'_0, \mathbf{V}'_0)$ for the target trajectory Γ and the values of the control parameters $\boldsymbol{\theta}$. Then the average battery drain of the group for the above task is given by

$$\bar{U}(\Gamma, \mathbf{Q}'_0, \mathbf{V}'_0, \boldsymbol{\theta}) = \frac{1}{T'N} \sum_{i=1}^N \int_0^{T'} |\mathbf{u}'_i(\mathbf{q}'_i(t'; \boldsymbol{\theta}), \mathbf{v}'_i(t'; \boldsymbol{\theta}), \mathbf{q}'_i(t'), \mathbf{v}'_i(t'); \boldsymbol{\theta})| dt'. \quad (73)$$

The quantities

$$\begin{aligned} \bar{Q}_{dev}(\Gamma, \mathbf{Q}'_0, \mathbf{V}'_0, \boldsymbol{\theta}) &= \frac{1}{T'N} \sum_{i=1}^N \int_0^{T'} |\mathbf{q}'_i(t'; \boldsymbol{\theta}) - \mathbf{q}'_i(t')| dt', \\ \bar{V}_{dev}(\Gamma, \mathbf{Q}'_0, \mathbf{V}'_0, \boldsymbol{\theta}) &= \frac{1}{T'N} \sum_{i=1}^N \int_0^{T'} |\mathbf{v}'_i(t'; \boldsymbol{\theta}) - \mathbf{v}'_i(t')| dt', \end{aligned} \quad (74)$$

characterize the overall quality of the group's formation during the task execution by measuring the average group's deviations from the target position and the target velocity, respectively. Therefore, we are interested in identifying parameters configurations $\boldsymbol{\theta}$ that, for given $\Gamma, \mathbf{Q}'_0, \mathbf{V}'_0$, yield the smallest possible values of $\bar{U}(\Gamma, \mathbf{Q}'_0, \mathbf{V}'_0, \boldsymbol{\theta})$ keeping $\bar{Q}_{dev}(\Gamma, \mathbf{Q}'_0, \mathbf{V}'_0, \boldsymbol{\theta})$ and $\bar{V}_{dev}(\Gamma, \mathbf{Q}'_0, \mathbf{V}'_0, \boldsymbol{\theta})$ below reasonable thresholds.

Simulations setting. As in the previous section, we consider a group of $N = 100$ agents in a 3-dimensional space and use the same parameters of the ambient forces. The initial positions \mathbf{Q}'_0 are drawn from the uniform distribution on the ball $B(\mathbf{q}'_l(0), 10)$, and the initial velocities \mathbf{V}'_0 are drawn from the truncated normal distribution with mean $\mathbf{q}'_l(0)$ and covariance matrix $0.25I_d$ supported on the ball $B(\mathbf{q}'_l(0), 0.5)$. We consider a trajectory Γ of the virtual leader that is composed of the following 3 stages: (1) a set of constant acceleration intervals required for the group to get from the initial location to the target location of interest (2) multiple rotations about the location of interest with constant angular speed (3) a set of constant acceleration intervals required for the group to get from the target location to the initial location. We assume that such a trajectory might be typical for practical applications. Finally, we choose the feasible region of the control parameters to be

$$\Theta = \{(\alpha', r'_0, \beta', v'_0) \in \mathbb{R}^4 \mid 0 \leq \alpha' \leq 5, 0 \leq r'_0 \leq 20, 0 \leq \beta' \leq 5, 0 \leq v'_0 \leq 2\}. \quad (75)$$

In an attempt to capture some general trends in the effects of the control parameters adjustments, we consider a grid Ξ of $26 \times 26 \times 26 \times 26$ equally spaced points on Θ , and perform a simulation using the target trajectory and the initial conditions specified above at each of the points of Ξ measuring (73) and (74). The projections of \bar{Q}_{dev} , \bar{V}_{dev} on the 1-dimensional spaces of the individual components of $\boldsymbol{\theta}$ are shown in Figure 4. An analogous plot for 2-dimensional spaces of pairs of components are shown in Figure 5.

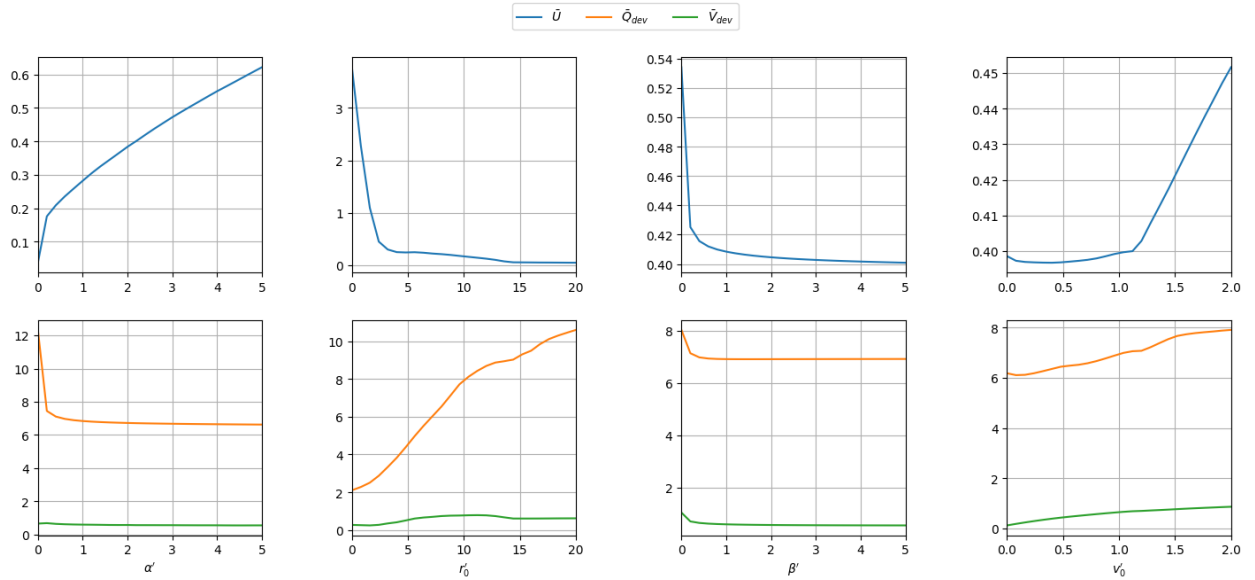


Figure 4: Values of \bar{U} , \bar{Q}_{dev} , \bar{V}_{dev} evaluated on Ξ . The projections of \bar{Q}_{dev} , \bar{V}_{dev} on the 1-dimensional spaces of the individual components of $\boldsymbol{\theta}$ are obtained by averaging over the remaining components.

Discussion of the results. As it could be seen from Figure 4, on average, adjustment of the magnitudes of the position and the velocity alignment forces have the opposite effects on

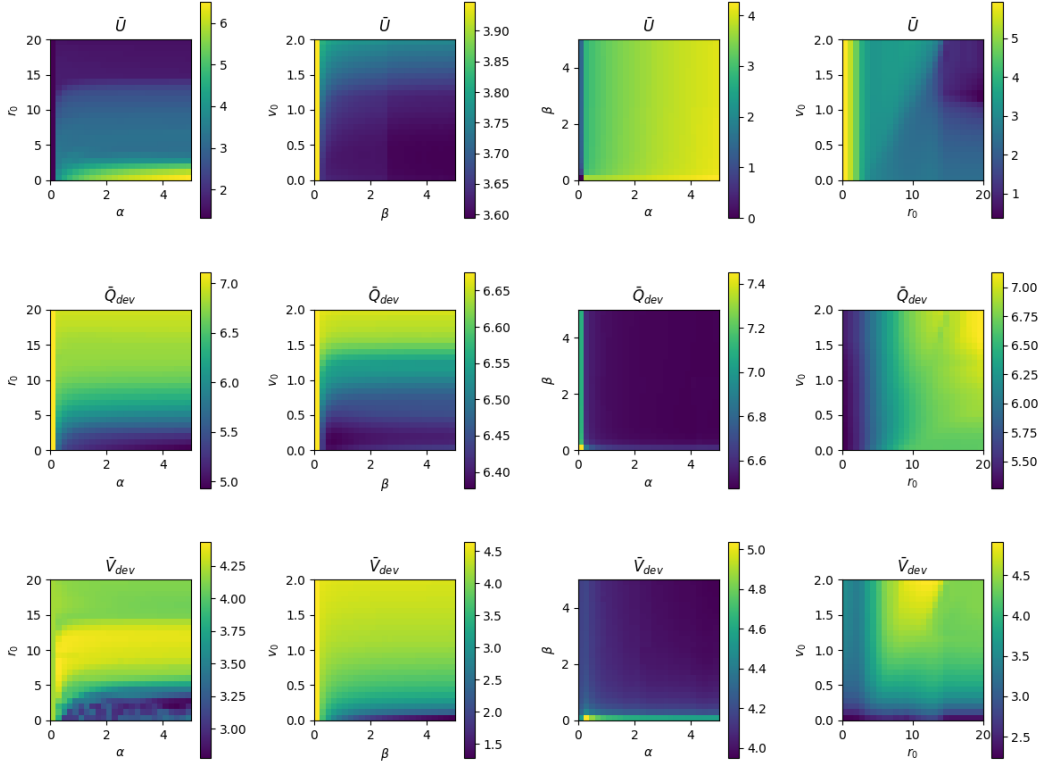


Figure 5: Values of \bar{U} , \bar{Q}_{dev} , \bar{V}_{dev} evaluated on Ξ . The projections of \bar{Q}_{dev} , \bar{V}_{dev} on the 2-dimensional spaces of the individual components of θ are obtained by averaging over the remaining components.

the battery drain: increasing α leads to an increase in the battery drain, whereas increasing β results in the battery being decreased. However, for $\alpha = 0$, the trend for β gets inverted, and \bar{U} becomes an increasing function of β (see Figure 5). Given that scenarios with $\alpha = 0$ are impractical since they might result in unacceptable spatial divergence, we assume that the position alignment force must be present in a typical scenario. Also, amplifying the magnitude of the velocity alignment force has a notable effect on both \bar{Q}_{dev} and \bar{V}_{dev} , whereas amplifying the magnitude of the position alignment force only has an effect on \bar{Q}_{dev} . Therefore, in a typical scenario, it turns out to be preferable to perform alignment of small deviations from the trajectory tracking with the help of the velocity alignment force. This will reduce the amount of work done by the position alignment force, which should only be activated when strong spatial deviations occur.

Aside from tuning the magnitude of the forces, their effect might be adjusted by config-

uring the corresponding activation radii r_0 and v_0 . Decreasing r_0 results in a tighter packing of the group being enforced and is naturally associated with the battery drain increase. It could be seen from Figure 4, that a significant jump this increase happens when the value of r_0 gets lower than approximately 3.5. Recall that the $r'_0 = 3.23$ is the radius that yields the optimal density $\rho = 0.74$. For the values of r'_0 that are less than this threshold, the position alignment force needs to permanently counteract the strong action of the ambient conservative, force significantly draining the battery. Thus, such values should be avoided as extremely inefficient, and, in general, r_0 should be set to the maximum value that can ensure the required control over the group spatial dispersion.

Although the plot of \bar{U} as a function of the activation threshold of the velocity alignment force v_0 has a global minimum that is distinct from zero, using in it in real-world applications is likely to be inefficient given the steady increase of \bar{Q}_{dev} and \bar{V}_{dev} with an increase in v_0 . Thus, the velocity alignment force must perform the tightest possible control both in the sense of having a higher magnitude and a higher activation radius.

Constrained optimization problem. Determining the actual values of the control parameters that are optimal for a particular task could be approached either as a constrained optimization problem where one finds the minimum of \bar{U} imposing upper bounds on \bar{Q}_{dev} and \bar{V}_{dev} or a multi-objective optimization problem where all the three quantities must be minimized simultaneously. Taking the former approach, we consider the problem

$$\begin{aligned} \min_{\boldsymbol{\theta} \in \Theta} \quad & \bar{U}(\Gamma, \mathbf{Q}'_0, \mathbf{V}'_0, \boldsymbol{\theta}) \\ \text{s.t.} \quad & \bar{Q}_{dev}(\Gamma, \mathbf{Q}'_0, \mathbf{V}'_0, \boldsymbol{\theta}) \leq Q_{max} \\ & \bar{V}_{dev}(\Gamma, \mathbf{Q}'_0, \mathbf{V}'_0, \boldsymbol{\theta}) \leq V_{max}, \end{aligned} \tag{76}$$

where $Q_{max}, V_{max} \geq 0$.

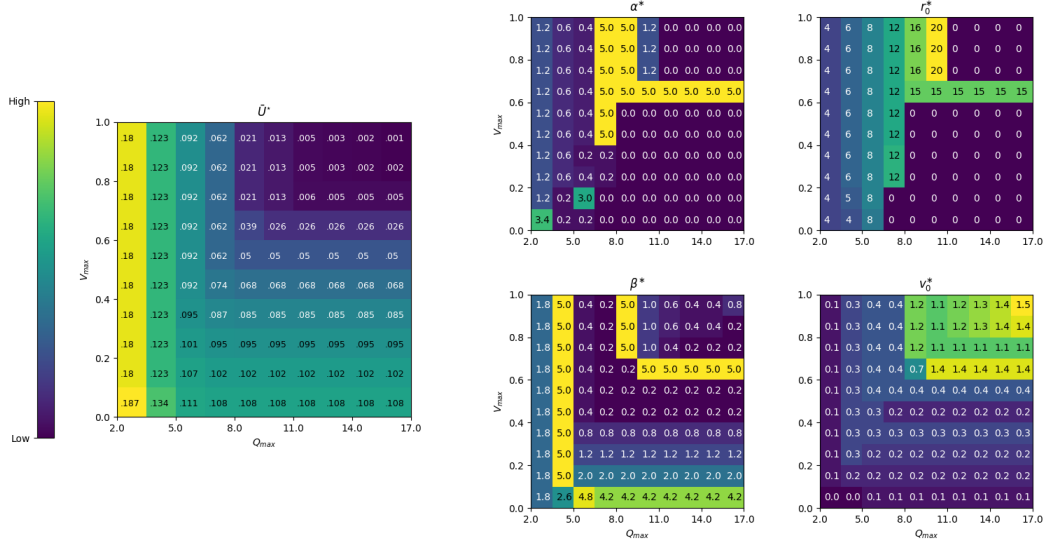
Putting $\Theta = \Xi$ in (76), we perform numerical solution of the resulting problem using the collected data described earlier. Figure 6 shows the solutions for ranges of values of Q_{max} and V_{max} .

Absence of monotonic trends in the plots for α and β seen in Figure 6 (b) demonstrates that the true geometry of $\bar{U}(\boldsymbol{\theta})$ as a surface in \mathbb{R}^4 is less trivial than it is suggested by Figure 4, where some geometrical features are canceled out by averaging.

The strictest enforcement of the flock formation is associated with the optimal parameter configuration is given by

$$\alpha' = 0.2, \quad r'_0 = 6.4, \quad \beta' = 1.4, \quad v'_0 = 0,$$

indicating that it is efficient to apply forces with both the intensity and the activation radii being low. In turn, relaxation of restrictions on Q_{max} V_{max} is associated with an increase in both intensity and activation radii. Depending on whether the upper bound on \bar{Q}_{dev} is relatively stronger than the one on V_{max} or vice versa, either position alignment or velocity alignment forces, respectively, should play a more important in the group alignment. At the same time, for some high values of Q_{max} V_{max} , the position alignment force might get



(a) Minimum values of \bar{U}

(b) Minimizers of \bar{U}

Figure 6: Solutions of the problem (76) with $\Theta = \Xi$.

negligibly small, whereas the velocity alignment force is always present, supporting our previous suggestion about its relevant importance.

8 Conclusion

We suggested a model of collective motion of a swarm of miniature robots that are steered by a virtual leader. Disregarding the physical nature of the forces that govern the dynamics, our model could be also seen as a generalization of the model of Olfati-Saber with non-linear navigational feedback forces. Although, in general, our system could not be guaranteed to be dissipative, we showed that, for navigational feedback forces that are bounded perturbations of linear ones, it possesses a global attractor that is characterized by flocking dynamics with bounded deviations of agents' trajectories from that of the virtual leader. We obtained explicit bounds on these deviations and showed how these bounds could be controlled with the tunable parameters of our navigational feedback forces. We also derived some mild conditions, under which all agents agree on a common velocity at an exponential rate.

When the system is dissipative, the attractor could contain non-equilibrium solutions, which cannot exist in the structural dynamics of the model of Olfati-Saber. We constructed examples of such solutions and obtained some sufficient conditions under which such solutions cannot exist.

We supported our theoretical findings by numerical simulations. We also provided a case study of the energy efficiency of the collective dynamics in our model and identified configurations of the control parameters that are optimal in this sense.

Appendices

Appendix A Proof of Lemma 1

Proof. Fix an open interval $I \subseteq \mathbb{R}$. Suppose $I \cap S$ is dense in I , but there exists $x_0 \in I$, such that $f(x_0) = \gamma > 0$. Clearly, $x_0 \notin I \cap S$, and therefore x_0 is a limit point of I . By continuity of f , there exists $\delta > 0$, such that $|f(x) - f(x_0)| = |f(x) - \gamma| < \gamma$, for all $x \in (x_0 - \delta, x_0 + \delta)$. Then $-\gamma < f(x) - \gamma$, and hence $f(x) > 0$ on $\tilde{I} = (x_0 - \delta, x_0 + \delta) \cap I$. That is, \tilde{I} doesn't contain any elements of $I \cap S$, which is a contradiction. \square

Appendix B Battery drain function

We assume that each agent is set in motion by a propeller that is powered by a DC motor connected to a battery. In this case, the battery drain is proportional to the input current I of the DC motor. In turn, the current is related to the torque \mathbf{T} produced by the motor as

$$|\mathbf{T}| = \frac{1}{k_T} I,$$

where k_T is the torque constant [26]. Finally, the self-propulsion force created by the thrust of the propeller is related to the torque as

$$|\mathbf{u}| = \frac{K_T |\mathbf{T}|}{K_Q D},$$

where D is the propeller's diameter, K_T and K_Q are torque coefficient and thrust coefficient, respectively, that are constants specific to geometric configuration of the propeller [10]. Thus, we get

$$\text{agent's battery drain} \propto I \propto |\mathbf{T}| \propto |\mathbf{u}|.$$

References

- [1] David Ball, Patrick Ross, Andrew English, Tim Patten, Ben Upcroft, Robert Fitch, Salah Sukkarieh, Gordon Wyeth, and Peter Corke. Robotics for sustainable broad-acre agriculture. In *Field and Service Robotics: Results of the 9th International Conference*, pages 439–453. Springer, 2015.
- [2] Jan Carlo Barca and Y Ahmet Sekercioglu. Swarm robotics reviewed. *Robotica*, 31(3):345–359, 2013.
- [3] C Miguel Barriuso Gutiérrez, José Martín-Roca, Valentino Bianco, Ignacio Pagonabarraga, and Chantal Valeriani. Simulating microswimmers under confinement with dissipative particle (hydro) dynamics. *Frontiers in Physics*, page 624, 2022.

- [4] Levent Bayındır. A review of swarm robotics tasks. *Neurocomputing*, 172:292–321, 2016.
- [5] Manuele Brambilla, Eliseo Ferrante, Mauro Birattari, and Marco Dorigo. Swarm robotics: a review from the swarm engineering perspective. *Swarm Intelligence*, 7:1–41, 2013.
- [6] Bernard Brogliato, Rogelio Lozano, Bernhard Maschke, Olav Egeland, et al. Dissipative systems analysis and control. *Theory and Applications*, 2:2–5, 2007.
- [7] Jerome Buhl, David JT Sumpter, Iain D Couzin, Joe J Hale, Emma Despland, Edgar R Miller, and Steve J Simpson. From disorder to order in marching locusts. *Science*, 312(5778):1402–1406, 2006.
- [8] Francesco Bullo, Jorge Cortés, and Sonia Martinez. *Distributed control of robotic networks: a mathematical approach to motion coordination algorithms*, volume 27. Princeton University Press, 2009.
- [9] Ada-Ioana Bunea and Rafael Taboryski. Recent advances in microswimmers for biomedical applications. *Micromachines*, 11(12):1048, 2020.
- [10] John Carlton. *Marine Propellers and Propulsion*. Butterworth-Heinemann, 2012.
- [11] Hakan Ceylan, Joshua Giltinan, Kristen Kozielski, and Metin Sitti. Mobile microrobots for bioengineering applications. *Lab on a Chip*, 17(10):1705–1724, 2017.
- [12] Jack Connor, Benjamin Champion, and Matthew A Joordens. Current algorithms, communication methods and designs for underwater swarm robotics: A review. *IEEE Sensors Journal*, 21(1):153–169, 2020.
- [13] John Horton Conway and Neil James Alexander Sloane. *Sphere packings, lattices and groups*, volume 290. Springer Science & Business Media, 2013.
- [14] Felipe Cucker and Steve Smale. Emergent behavior in flocks. *IEEE Transactions on automatic control*, 52(5):852–862, 2007.
- [15] András Czirók, Eshel Ben-Jacob, Inon Cohen, and Tamás Vicsek. Formation of complex bacterial colonies via self-generated vortices. *Physical Review E*, 54(2):1791, 1996.
- [16] Yuan-Shun Dai, Michael Hinchey, Manish Madhusoodan, James L Rash, and Xukai Zou. A prototype model for self-healing and self-reproduction in swarm robotics system. In *2006 2nd IEEE international symposium on dependable, autonomic and secure computing*, pages 3–10. IEEE, 2006.
- [17] Ali Dorri, Salil S Kanhere, and Raja Jurdak. Multi-agent systems: A survey. *Ieee Access*, 6:28573–28593, 2018.

- [18] Dmitry A Fedosov, Wenxiao Pan, Bruce Caswell, Gerhard Gompper, and George E Karniadakis. Predicting human blood viscosity in silico. *Proceedings of the National Academy of Sciences*, 108(29):11772–11777, 2011.
- [19] Chris Godsil and Gordon F Royle. *Algebraic graph theory*, volume 207. Springer Science & Business Media, 2001.
- [20] Sabine Hauert, Jean-Christophe Zufferey, and Dario Floreano. Evolved swarming without positioning information: an application in aerial communication relay. *Autonomous Robots*, 26:21–32, 2009.
- [21] Y Hayakawa. Spatiotemporal dynamics of skeins of wild geese. *Europhysics Letters*, 89(4):48004, 2010.
- [22] Charlotte K Hemelrijk and Hanspeter Kunz. Density distribution and size sorting in fish schools: an individual-based model. *Behavioral Ecology*, 16(1):178–187, 2005.
- [23] FH Heppner. Three-dimensional structure and dynamics of bird flocks. *Animal groups in three dimensions*, pages 68–89, 1997.
- [24] PJ Hoogerbrugge and JMVA Koelman. Simulating microscopic hydrodynamic phenomena with dissipative particle dynamics. *Europhysics letters*, 19(3):155, 1992.
- [25] Wenying Hou, Minyue Fu, Huanshui Zhang, and Zongze Wu. Consensus conditions for general second-order multi-agent systems with communication delay. *Automatica*, 75:293–298, 2017.
- [26] A Hughes and B Drury. *Electric motors and drives: fundamentals, types and applications, 4th edn.* Newnes. Oxford, 2013.
- [27] Christoph Junghans, Matej Praprotnik, and Kurt Kremer. Transport properties controlled by a thermostat: An extended dissipative particle dynamics thermostat. *Soft Matter*, 4(1):156–161, 2008.
- [28] Matz Larsson. Why do fish school? *Current Zoology*, 58(1):116–128, 2012.
- [29] Joseph LaSalle. Some extensions of liapunov’s second method. *IRE Transactions on circuit theory*, 7(4):520–527, 1960.
- [30] Huan Lei and George Em Karniadakis. Quantifying the rheological and hemodynamic characteristics of sickle cell anemia. *Biophysical journal*, 102(2):185–194, 2012.
- [31] Reza Olfati-Saber. Flocking for multi-agent dynamic systems: Algorithms and theory. *IEEE Transactions on automatic control*, 51(3):401–420, 2006.
- [32] W Pan, IV Pivkin, and GE Karniadakis. Single-particle hydrodynamics in dpd: A new formulation. *Europhysics Letters*, 84(1):10012, 2008.

- [33] Alexander Panchenko, Denis F Hinz, and Eliot Fried. Spatial averaging of a dissipative particle dynamics model for active suspensions. *Physics of Fluids*, 30(3):033301, 2018.
- [34] Julia K Parrish, Steven V Viscido, and Daniel Grunbaum. Self-organized fish schools: an examination of emergent properties. *The biological bulletin*, 202(3):296–305, 2002.
- [35] Jiahu Qin, Qichao Ma, Yang Shi, and Long Wang. Recent advances in consensus of multi-agent systems: A brief survey. *IEEE Transactions on Industrial Electronics*, 64(6):4972–4983, 2016.
- [36] Wei Ren and Randal W Beard. Consensus algorithms for double-integrator dynamics. *Distributed Consensus in Multi-vehicle Cooperative Control: Theory and Applications*, pages 77–104, 2008.
- [37] Pawel Romanczuk and Lutz Schimansky-Geier. Mean-field theory of collective motion due to velocity alignment. *Ecological Complexity*, 10:83–92, 2012.
- [38] Joan Saez-Pons, Lyuba Alboul, Jacques Penders, and Leo Nomdedeu. Multi-robot team formation control in the guardians project. *Industrial Robot: An International Journal*, 37(4):372–383, 2010.
- [39] Felix Schill, Alexander Bahr, and Alcherio Martinoli. Vertex: A new distributed underwater robotic platform for environmental monitoring. In *Distributed Autonomous Robotic Systems: The 13th International Symposium*, pages 679–693. Springer, 2018.
- [40] Melanie Schranz, Martina Umlauft, Micha Sende, and Wilfried Elmenreich. Swarm robotic behaviors and current applications. *Frontiers in Robotics and AI*, page 36, 2020.
- [41] Metin Sitti. *Mobile microrobotics*. MIT Press, 2017.
- [42] Andrey Sokolov, Igor S Aranson, John O Kessler, and Raymond E Goldstein. Concentration dependence of the collective dynamics of swimming bacteria. *Physical review letters*, 98(15):158102, 2007.
- [43] Housheng Su, Guanrong Chen, Xiaofan Wang, and Zongli Lin. Adaptive second-order consensus of networked mobile agents with nonlinear dynamics. *Automatica*, 47(2):368–375, 2011.
- [44] Housheng Su, Xiaofan Wang, and Zongli Lin. Flocking of multi-agents with a virtual leader part ii: With a virtual leader of varying velocity. In *2007 46th IEEE Conference on Decision and Control*, pages 1429–1434. IEEE, 2007.
- [45] Housheng Su, Xiaofan Wang, and Zongli Lin. Flocking of multi-agents with a virtual leader. *IEEE transactions on automatic control*, 54(2):293–307, 2009.

- [46] Ying Tan and Zhong-yang Zheng. Research advance in swarm robotics. *Defence Technology*, 9(1):18–39, 2013.
- [47] Herbert G Tanner, Ali Jadbabaie, and George J Pappas. Flocking in fixed and switching networks. *IEEE Transactions on Automatic control*, 52(5):863–868, 2007.
- [48] Roger Temam. *Infinite-dimensional dynamical systems in mechanics and physics*, volume 68. Springer Science & Business Media, 2012.
- [49] John Toner and Yuhai Tu. Flocks, herds, and schools: A quantitative theory of flocking. *Physical review E*, 58(4):4828, 1998.
- [50] Tamás Vicsek, András Czirók, Eshel Ben-Jacob, Inon Cohen, and Ofer Shochet. Novel type of phase transition in a system of self-driven particles. *Physical review letters*, 75(6):1226, 1995.
- [51] Tamás Vicsek and Anna Zafeiris. Collective motion. *Physics reports*, 517(3-4):71–140, 2012.
- [52] Zhengjia Wang, Hsuan-Yi Chen, Yu-Jane Sheng, and Heng-Kwong Tsao. Diffusion, sedimentation equilibrium, and harmonic trapping of run-and-tumble nanoswimmers. *Soft Matter*, 10(18):3209–3217, 2014.
- [53] Guanghui Wen, Zhisheng Duan, Zhongkui Li, and Guanrong Chen. Flocking of multi-agent dynamical systems with intermittent nonlinear velocity measurements. *International Journal of Robust and Nonlinear Control*, 22(16):1790–1805, 2012.
- [54] S. Wiggins. *Introduction to Applied Nonlinear Dynamical Systems and Chaos*. Texts in Applied Mathematics. Springer New York, 2003.
- [55] Song Xiao, Hsuan-Yi Chen, Yu-Jane Sheng, and Heng-Kwong Tsao. Induced polar order in sedimentation equilibrium of rod-like nanoswimmers. *Soft Matter*, 11(12):2416–2422, 2015.
- [56] Lidong Yang, Jiangfan Yu, Shihao Yang, Ben Wang, Bradley J Nelson, and Li Zhang. A survey on swarm microrobotics. *IEEE Transactions on Robotics*, 38(3):1531–1551, 2021.
- [57] Wenwu Yu, Guanrong Chen, and Ming Cao. Distributed leader–follower flocking control for multi-agent dynamical systems with time-varying velocities. *Systems & Control Letters*, 59(9):543–552, 2010.